

“Finite Element Analysis of Geogrid Reinforced Soil Wall”

A DISSERTATION

SUBMITTED IN PARTIAL FULFILLMENT
FOR REQUIREMENT OF THE DEGREE OF
MASTER OF TECHNOLOGY

IN

**CIVIL ENGINEERING
(Geotechnical Engineering)**

Submitted by
AJAY KUMAR
(2K20/GTE/01)

Under the supervision of

Prof. ASHOK KUMAR GUPTA



CIVIL ENGINEERING DEPARTMENT
DELHI TECHNOLOGICAL UNIVERSITY
Bawana road, Delhi – 110042

May - 2022

CANDIDATE'S DECLARATION

I, **Ajay Kumar, 2K20/GTE/01**, student of M.Tech (Civil Engineering), hereby declare that the project dissertation titled “**Finite Element Analysis of Geogrid Reinforced Soil Wall**” is submitted to the Department of Civil Engineering, Delhi Technological University, Delhi, by me in partial fulfillment of requirement for the award of degree of **Master of Technology (Geotechnical Engineering)**. This thesis is original work done by me and not obtained from any source without proper citation. This project work has not previously formed the basis for award of any degree, diploma, fellowship or other similar title or recognition.

Place: Delhi

Date: 30/05/2022

AJAY KUMAR

(2K20/GTE/01)

CIVIL ENGINEERING DEPARTMENT
DELHI TECHNOLOGICAL UNIVERSITY
Bawana road, Delhi – 110042



CERTIFICATE

I hereby certify that project dissertation titled “**Finite Element Analysis of Geogrid Reinforced Soil Wall**” submitted by **Ajay Kumar, 2K20/GTE/01**, Department of Civil Engineering, Delhi Technological University, Delhi, in partial fulfillment for the award of degree of Master of Technology, is a project work carried out by the student under my supervision. To the best of my knowledge, this work has not been submitted in part or full for any degree or diploma to this university or elsewhere.

Supervisor

Prof. ASHOK KUMAR GUPTA

CIVIL ENGINEERING DEPARTMENT

Delhi Technological University,

Delhi-110042

ACKNOWLEDGEMENTS

I express my deep gratitude and indebtedness to **Prof. Ashok Kumar Gupta**, Department of Civil Engineering, DTU, Delhi, for his guidance, and valuable feedback throughout this project work. His able knowledge and supervision with unswerving patience fathered my project work at every stage, for without his encouragement, the fulfilment of task would have been impossible and difficult.

I wish to express my gratitude towards our Head of Department, **Prof. V. K. Minocha**, Department of Civil Engineering, DTU, Delhi, for showing interest and providing help throughout the period of my project work.

I am genuinely appreciative to all my Friend for their support and suggestions during my work. Lastly, I would like to thank the Almighty GOD and my parents, whose committed and untiring efforts towards me have brought me at this stage of my life.

AJAY KUMAR

(2K20/GTE/01)

Date: 30/05/2022

ABSTRACT

Geogrid reinforced soil wall (GRSW) are the cost effective retaining wall which is mostly used now days. GRS walls have become more popular because of their uses over the retaining walls such as flexibility, ease in construction, lower cost than normal walls. This basically reduce the differential settlement in foundation due to the variation of surcharge loading. This study is mainly based on settlement and stability calculation on backfill soil. The behavior of lower GRS wall has seen below the abutment in this study. Geogrids are used to safe the structure at various loading conditions to reduce settlement and increase the stability of structure. Geogrids also used to mitigate the displacement in the soil wall. Finite element analysis method has been used by commercially available software PLAXIS 2D. In which the plane strain model with 15 noded elements was defined to simulate the problem. By use of this, effect of different surcharge loading and bridge load applied on the lower GRS wall to see the behavior of soil structure.

Keywords: Surcharge loading, Lower GRS wall, Finite element method, bridge abutment, settlement, safety analysis, PLAXIS 2D.

CONTENTS

TOPIC	PAGE NO.
Declaration by candidate	ii
Certificate	iii
Acknowledgement	iv
Abstract	v
Figures	viii
Tables	ix
Graphs	x
Introduction	01-03
Origin of project	
Objective of project	
Review of Literature	04-10
Effects of backfill	
Effects of geogrids in Lower GRS wall	
Effects of abutment on Lower GRS wall	
Effects of reinforced stiffness and compaction of backfill	
Theory	11-14
Finite element method (PLAXIS 2D)	
Geogrids	
Methodology	15-18
Concept model	
Model for study in PLAXIS 2D	
Phase construction in PLAXIS 2D	
Results and Discussion	19-41
Deformation analysis in PLAXIS 2D	
Safety analysis in PLAXIS 2D	
Conclusion and scope of study	42-43
References	44-45

FIGURES

Figure	Description	Page No.
Figure 1.1	Lower GRS wall (Hejleh et al. ,2002)	2
Figure 1.2	Use of Lower GRS wall in Narayanpuram road bridge	2
Figure 2.1	Differential settlement in backfill soil (Zheng et al. ,2016)	4
Figure 2.2	Differential settlement in backfill soil (Zheng et al. ,2016)	5
Figure 2.3	The two-part wedge planer failure geometry	5
Figure 2.4	Free body diagram for wall facing	6
Figure 2.5	Variation of failure line in Mohr-Coulomb	7
Figure 2.6	Prototype model (Bathrust, 2009)	9
Figure 3.1	Iterative procedure for model load control (Guler et al. ,2012)	12
Figure 3.2	Iterative procedure for arc load control	13
Figure 3.3	Photos of geogrids	13
Figure 3.4	Photos of GRS extensible reinforcement	14
Figure 3.5	Typical wrapped face structure of GRS	14
Figure 4.1	Model used for probabilistic analysis	15
Figure 4.2	Model used in PLAXIS 2D for analysis	16
Figure 5.1	Deformation without geogrids	19
Figure 5.2	Wall displacement without geogrids	19
Figure 5.3	Deformed mesh of model without geogrids	20
Figure 5.4	Stresses mesh without geogrids	20
Figure 5.5	Deformation with geogrids	21
Figure 5.6	Wall displacement with geogrids	21
Figure 5.7	Deformed mesh of model with geogrids	22
Figure 5.8	Stresses mesh with geogrids	22

Figure 5.9	Deformation without geogrids	23
Figure 5.10	Wall displacement without geogrids	23
Figure 5.11	Deformation mesh of model without geogrids	24
Figure 5.12	Stresses mesh without geogrid	24
Figure 5.13	Deformation with geogrids	25
Figure 5.14	Wall displacement with geogrids	25
Figure 5.15	Deformation mesh with geogrids	26
Figure 5.16	Stresses mesh with geogrids	26
Figure 5.17	Deformation without geogrids	27
Figure 5.18	Wall displacement without geogrid	27
Figure 5.19	Deformed mesh of model without geogrid	28
Figure 5.20	Stresses mesh without geogrid	28
Figure 5.21	Deformation with geogrids	29
Figure 5.22	Wall displacement with geogrids	29
Figure 5.23	Deformed mesh with geogrids	30
Figure 5.24	Stresses mesh with geogrids	30
Figure 5.25	Deformation without geogrids	31
Figure 5.26	Displacement of wall without geogrids	31
Figure 5.27	Deformed mesh without geogrids	32
Figure 5.28	Stresses mesh without geogrids	32
Figure 5.29	Deformation with geogrids	33
Figure 5.30	Wall displacement with geogrids	33
Figure 5.31	Deformed mesh with geogrids	34
Figure 5.32	Stresses mesh with geogrids	34

TABLES

Table No.	Description
Table 2.1	Parameters used by Xiao et al. (2020)
Table 4.1	Input parameters used in modeling
Table 4.2	Properties of reinforcement used in modeling
Table 4.3	Properties of concrete block in modeling
Table 5.1	Load variation with factor of safety without geogrids
Table 5.2	Load variation with factor of safety with and without geogrids
Table 5.3	Load variation with displacement without geogrids
Table 5.4	Load with displacement with geogrids
Table 5.5	Displacement variation with factor of safety with geogrids

GRAPHS

Graph	Description
Graph 5.1	Surcharge load v/s FOS for without geogrids
Graph 5.2	Surcharge load v/s FOS for with and without geogrid
Graph 5.3	Load v/s displacement for without for without
Graph 5.4	Load v/s displacement with geogrid
Graph 5.5	Displacement v/s FOS with geogrids
Graph 5.6	Surcharge load v/s deflection

CHAPTER 1 - INTRODUCTION

ORIGIN OF PROJECT

Soil reinforcement are used geotextiles, geogrids, metallic strips, and other materials to support the soil. Because the reinforcement is immersed in the ground, it produces almost no tension, allowing the wall to be stable at higher heights. The shear resistance formed between both the soil and reinforcement enhances the shear strength of the soil. Because pore water impacts the shear capacity of cohesive soils, the major of today's construction is performed using free drainage granular soils. These walls are built to provide both internal and external stability. Internal stability includes assessing tension and pullout strength in reinforcing elements, while external stability includes overturning, sliding, and load carrying failure. GRS walls are also used in transportation systems to sustain backfill dirt, roadway construction, and traffic loads. The rising use of soil reinforcement is encouraged by factors such as cost, aesthetics, convenience of construction, greater structural behaviour, and the ability to endure differential settlement.

The following are some examples of real-time soil reinforcement applications:

- Retaining structures for soil
- Abutments and side walls of bridges
- Railway and road embankments
- Slope failure repair
- Slope cutting repairs

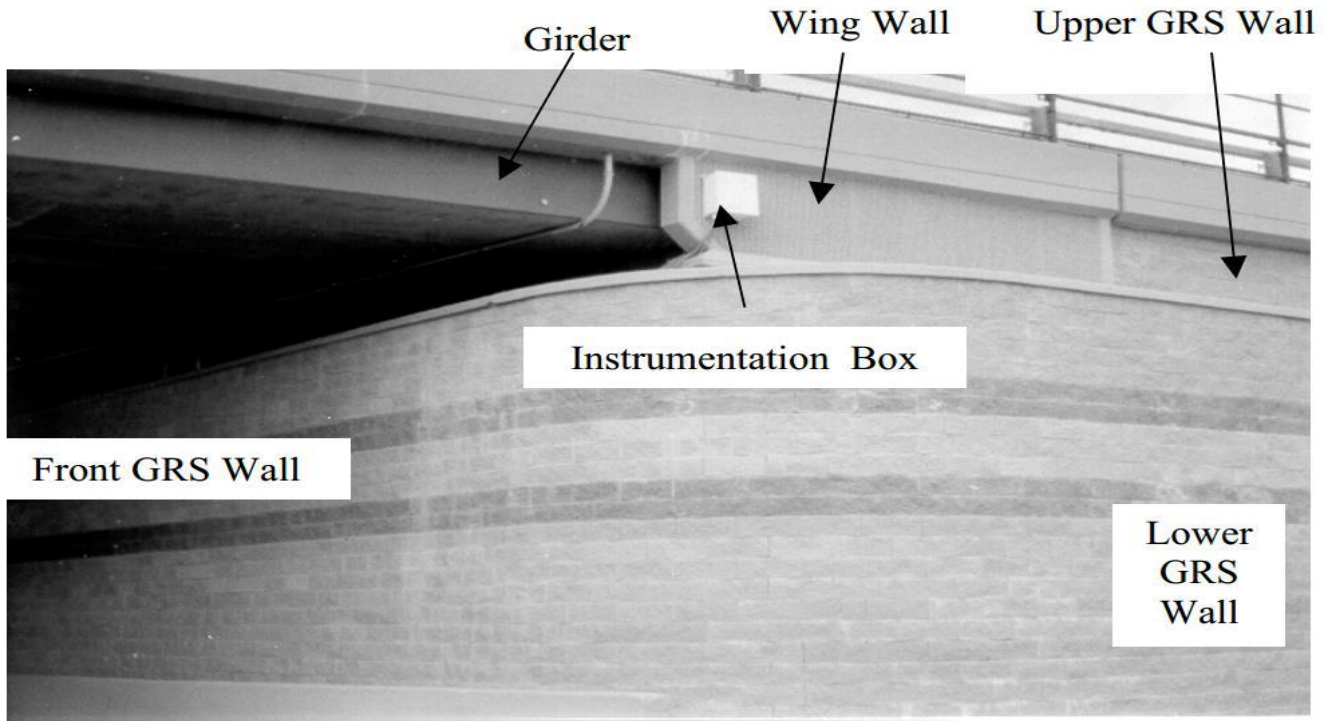


Figure 1.1 Lower GRS Wall (Hejleh et al., 2002)



Figure 1.2 Use of Lower GRS Wall in Narayanapuram Road bridge, Chebrolu (Andhra Pradesh)

The stability and deformation analysis in this work was done utilising the finite element technique (FEM). The behavior of the wall is investigated with a surcharge imposed to the footing laying on the back of the wall facing a setback distance. The angle of frictional resistance of the backfill soil, the length of reinforcement, the relative density of the backfill, the amount of reinforcement applied, and the interaction coefficient with both reinforcement as well as the backfill were studied. The output of the FEM analysed for the future scope of the study. Failure and deformation analyses were performed for a variety of examples with varying setback distances and backfill soil conditions. Finite element analysis must be undertaken to show that the observed and literature values are in good agreement. The friction and strain interaction between both the fill material and soil reinforcement is what provides the wall construction its strength. The main objective of the thin wall face is to prevent structural backfill erosion. As a result, a versatile gravity structure capable of carrying a wide range of heavy weights has been developed.

OBJECTIVE OF PROJECT

The objectives of current study are as follows:

- I. Calculate the deformation analysis of Geogrid reinforced soil wall.
- II. Calculate the safety analysis of Geogrid reinforced soil wall.
- III. Study the load behavior on the lower GRS Wall by use of geogrids and the properties of backfill soil.

CHAPTER 2 – LITRATURE REVIEW

For this study, various literature reviews are described for deformation and safety factor. Other factors influencing of a lower GRS walls include cohesiveness, angle of friction, and backfill soil unit weight, and the impact of various aspects have been recorded in the literature. Performance of the lower GRS wall as a bridge abutment is also covered in the current literature.

2.1 EFFECT OF BACKFILL

Zheng et al. (2016) has studied influence of backfill and cohesive on the reinforced soil wall. According to the findings, horizontal wall deflections were decreased by up to 50% and stress pressures were considerably reduced provided cohesive backfill was used. Because backfill soil variables re-present conservative values for strength and stiffness, rather substantial soil compression occurs in the baseline situation (Duncan et al. 1980). The settlement of the bridge footing as a result of additional construction following footing placement is 67.3mm. After bridge footing laying, the equivalent foundation soil settlement is 14.8 mm. As a result, the backfill soil for lower wall has a vertical compression of 53.6 mm.

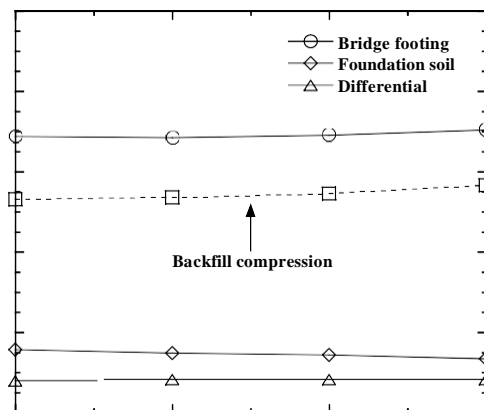


Figure 2.1 differential settlement in backfill soil (Zheng et al. 2016)

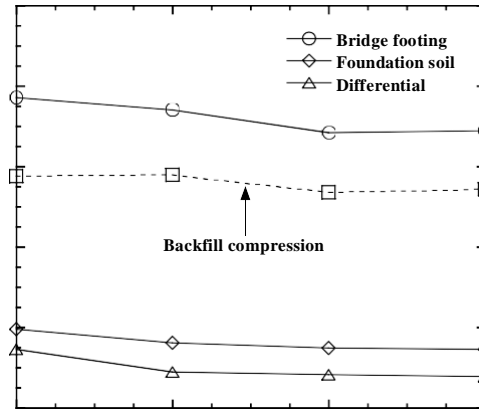


Figure 2.2 differential settlement in backfill soil (Zheng et al. 2016)

Peng et al. (2019) investigated the failure, parametric simulation and the finite element analysis were used, reinforced soil walls using extensible reinforcing mechanisms. Many different models were tested, each with different reinforcement spacing, backfill soil and length. When design loads are exceeded, the direct sliding mode is the main failure mechanism for walls for both granular and cohesive backfill soil. Tensile loads were lower in cohesive backfill than in granular backfill. While granular fill material, cohesive backfill walls might have no shearing strain concentrating region at the end of construction under working load conditions.

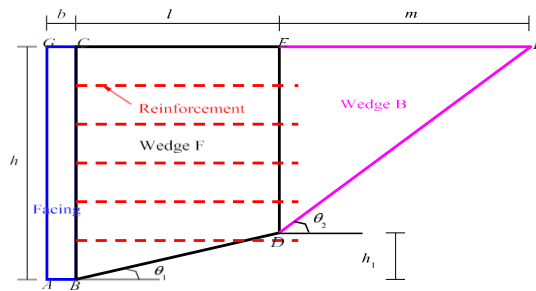


Figure 2.3 The two-part wedge planar failure geometry

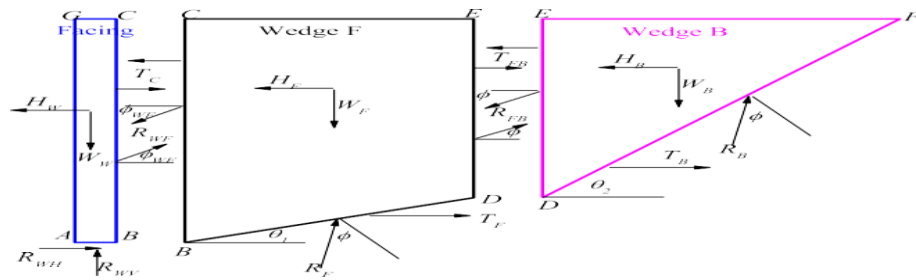


Figure 2.4 Free body diagram for wall facing

Following equation used for this FBD analysis

$$RFB \cos \phi + TB - TFB - HB - RB \sin(\theta_2 - \phi) = 0$$

$\sum F_y = 0$ (Wedge B in vertical direction)

$$RFB \sin \phi + RB \cos(\theta_2 - \phi) - WB = 0$$

$\sum F_x = 0$ (Wedge F in horizontal direction)

$$RWF \cos \phi + WF + RF \sin(\phi - \theta_1) + TF + TFB - TC - HF - RFB \cos \phi = 0$$

$\sum F_y = 0$ (Wedge F in vertical direction)

$$RWF \sin \phi + WF + RF \cos(\phi - \theta_1) - WF - RFB \sin \phi = 0$$

Yu et al. (2015) investigated a Japanese LGRS wall strengthened with geogrids strips. The results reveal that as the backfill soil stiffness rises, the tension loads in the wire strips, as well as the vertically face load at the toe, decrease.

2.2 EFFECTS OF GEOGRIDS IN LOWER GRS WALL

Xiao et al. (2020) studied on the BR-101 roadway in Santa Catarina, Brazil, the behavior of reinforced bridge structure near an existing road embankment and the grid. The bridge's foundation is built of organic soft clay, and backfill soil is supported by unidirectional geogrid layers. The faster speed of embankment construction and the positioning of stiffer reinforcing levels all along embankment axis caused the side slopes from one of the retaining walls to collapse. By building a berm along the side slope, this failure can be prevented. The use of reinforcement layers reduced lateral foundation soil displacement and minimised damage to existing structures.

Table: 2.1 Parameters used by Xiao et al. (2020)

Backfill properties Friction angle, ϕ (degree)	40, 45, 46, 47
Spacing of reinforcement, S_v (m)	0.25, 0.45, 0.65, 0.85
Length of reinforcement (H is height of abutment)	0.3H, 0.4H, 0.7H, H
Reinforcement stiffness, J (kN/m)	400, 800, 1200, 2400
Abutment height, H (m)	3, 4, 5, 6, 9
Facing batter, β (degree)	0, 2, 4, 8
Concrete footing width, B (m)	0.5, 0.7, 1, 1.5, 2, 3
Surcharge load (kPa)	50, 100, 200, 400

The elastic deformation and settling are moderate and do not fully describe geo-mechanical principles. The equations' coefficients are based on a lot of simulations with input variables that vary within the specified range. Infill friction direction of 40° to 47° , reinforcement distance of 0.25–0.85 m, prestressing length of 0.4H to H, reinforcement initial stiffness of 400–2400 kN/m, abutment height of 3–9 m, facing batter of 0–8°, concrete footing width of 0.5–3 m, and surcharge loading of 50–400 kPa. When variables in between these range are used, the correctness of the equation is not evaluated.

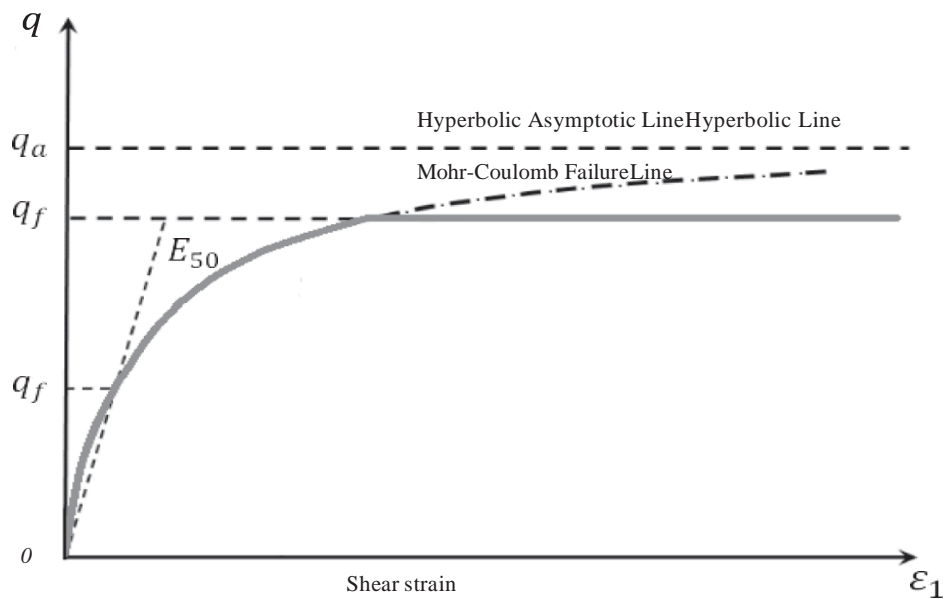


Figure 2.5 Variation of failure line in Mohr-Coulomb model (Xiao et al. ,2020)

Alam et al. (2019) Studied the efficiency of GRS bridge abutments was numerically studied under static footing loading. Bridge contact friction factor, backfill soil cohesiveness, backfill soil relative compacted, reinforcement distance, length, and rigidity, and bridge load were all evaluated. Backfill soil comparable compacted, reinforcing gap, and bridge loads have a greater impact on laterally side displacements and foundation footing settlements.

Grien et al. (2010) analysed in PLAC2D the effect of thermal stress of an integrated bridge deck on the a retaining structures earth (MSE) wall, with an emphasis on generated tension in reinforcement and displacement of the face wall due to bridge movement. The horizontal movement of the bridge affects the vertically tension beneath the footing. When opposed to integral bridge abutments, that have a lateral restraint provided by the bridge deck, typical bridge abutments migrate inward. This unforeseen deflection is one of the reasons for the greater shear strain and lateral movement.

Hejleh et al. (2002) studied Near Denver, Colorado, USA, GRS wall monitor a two-span bridge and approaching traffic. They studied the assessment of the effect of the Founders/Meadows bridges under service loads using displacement data obtained through surveying, gauges, and a road profiler. The observed displacements are smaller than expected, according to the data. There is not any indications of differential deformations or the bridge bump. Outward displacements after construction have been minimal throughout time and are diminishing.

2.3 EFFECTS OF ABUTMENT ON LOWER GRS WALL

Hatami and Doger (2020) studied large solid concrete blocks for the facing of GRS abutments could improve their load-bearing capability greatly when compared to abutments made of wood. They also signify the use of geogrids with wood is not so much effective than geogrids with the concrete. Which develops the best utilization of geogrids as retaining wall in concrete bridge structure.

Mirmoradi (2021) studied mechanically stabilized earth (MSE) walls provide various advantages over other traditional retaining structures, including lower costs, greater flexibility, improved aesthetics, as well as the possibility of reducing "bridge bumps" caused by foundation settlement in pile-supported abutments.

Mirmoradi et al. (2014) analysed numerical analysis on GRS walls with segmented block facing and base restraint. They discovered that under free defined with constant reinforcing stiffness, reinforcement tension was affected by facing rigidity and remained constant. The lateral toe stress for the fixed support and the tension generated in reinforcement are both a product of facing stiffness.

Bathrust at el.(2009) studied that compaction has a significant effect on the relative of building components outwards wall deformation and horizontally earth load at the toe at the end of construction in GRS walls. The impact of compact was mitigated by using an external surcharge. After pre-loading, the instantaneous and long-term residual deflections in the wall were reported to be relatively modest changes in the structure.

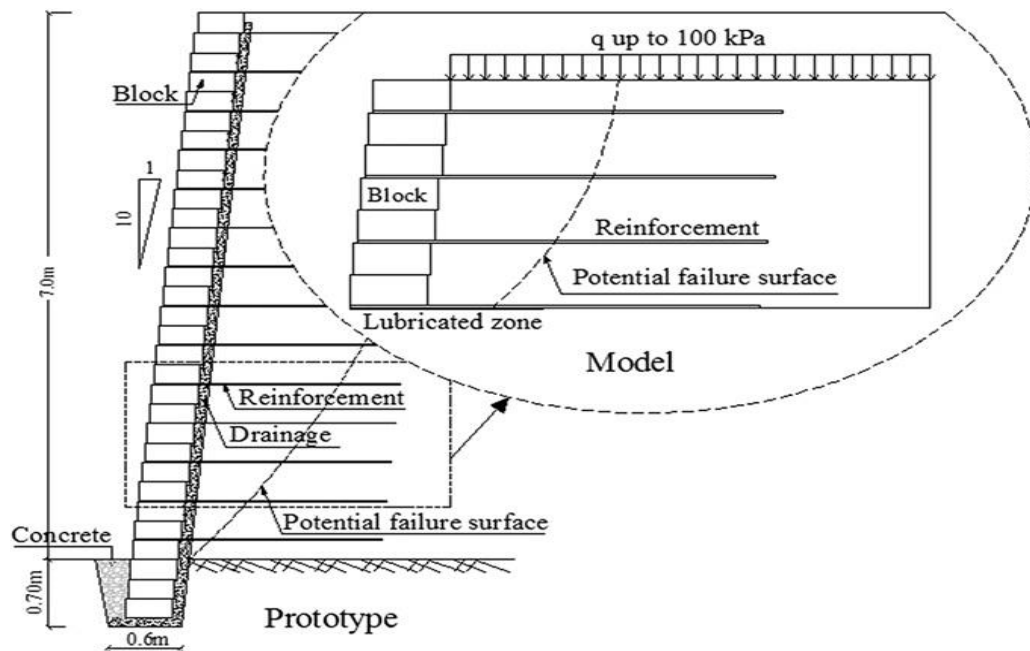


Figure 2.6 Prototype model (Bathrust, 2009)

2.1.4 EFFECTS OF REINFORCED STIFFNESS AND COMPACTION OF BACKFILL

Adams and nicks (2018) studied total of 21 wall models with various reinforcing stiffness levels. The findings suggested that using less stiff reinforcement layers at smaller spacings is preferable than using stiffer reinforcement layers at larger spacings for minimising facing distortion.

Shangchuan yang (2016) studied the reinforcement in the strongly compacted wall has higher mobilised tension in soil structure than the reinforcement in the light compacted wall. The connection load was lower in the severely compacted wall than it was in the light-compacted wall.

Biabani et al. (2016) studied by using finite element software, researchers evaluated the Under cyclic stress conditions, the displacement performance of a railway slipper on a geosynthetic reinforced granular materials. A nonlinear elastic material model was utilised for the geocell element, with elastic properties obtained from laboratory investigations.

CHAPTER-3 THEORY

3.1 FINITE ELEMENT METHOD (PLAXIS 2D)

PLAXIS 2D is a commercial finite element tool for 2-D study of deformation and stability problems in geotechnical engineering. It has a variety of capabilities to cope with complex geotechnical constructions. The modelling in this study was done with a 2-D planar strain condition and a 15-noded triangular element for the materials under consideration.

For soil modelling, the Mohr-Coulomb model is used. This model requires five input parameters: Young's modulus (E in kN/m^2), Poisson's ratio, cohesion (c in kN/m^2), angle of internal friction (in degrees), and dilatancy angle (in degrees). The mesh has been constructed, which divides the entire model into a number of discrete triangular parts, once the geometry has been fully described and the material characteristics have been assigned to all clusters and structural items. The displacements (u_x and u_y) are determined at the nodes throughout the computation process, and these nodes can be pre-selected for the creation of load-displacement curves. Rather than nodes, the stresses and strains are calculated at Gaussian integration points or stress points (Guler et. al 2012).

The ϕ - c reduction approach is used to calculate the factor of safety (FOS) from PLAXIS 2D. The strength parameters ϕ and c of the soil are gradually lowered in this method until failure occur. The strength parameters are automatically reduced throughout calculation until the final calculation step, resulting in a fully established failure mechanism. When interfaces are employed, this strength is likewise diminished. In PLAXIS the total multiplier ΣMsf is used to define the soil strength parameters at a given stage and is define as follows

$$\Sigma Msf = \frac{\tan \phi_{input}}{\tan \phi_{reduction}} = \frac{c_{input}}{c_{output}}$$

The attributes specified in the material sets are denoted by the subscript 'input,' and the reduced values used in the analysis are denoted by the subscript reduced. The technique load advancement number of

steps defined in PLAXIS 2D is used to calculate the phi-c reduction. Numerical limit analysis finds for the solution directly by mixing optimization techniques and rigorous plasticity theory, whereas elasto-plastic FE analysis requires many iterations to arrive at a ULS solution.

It must be checked always whether the final step has resulted in a fully developed failure mechanism, in this case the FOS is given by:

$$SF = \text{available strength} / \text{strength at failure}$$

$$= \text{value of } \Sigma Msf \text{ at failure}$$

The calculation should be performed with a higher number of steps if the failure mechanism is not fully developed. The arc-length control approach, which is by default selected for plastic calculation or phi-c reduction calculation to acquire the collapse loads, is available in PLAXIS for load-controlled calculations. Figure (a) shows the iteration technique when arc-length control is not employed and the collapse load is approaching. The algorithm will not converge to a solution in this scenario; hence the calculation will continue to iterate. The PLAXIS will automatically measure the fraction of external stress that must be applied for the structure to collapse if the arc-length control is selected (Figure (b)).

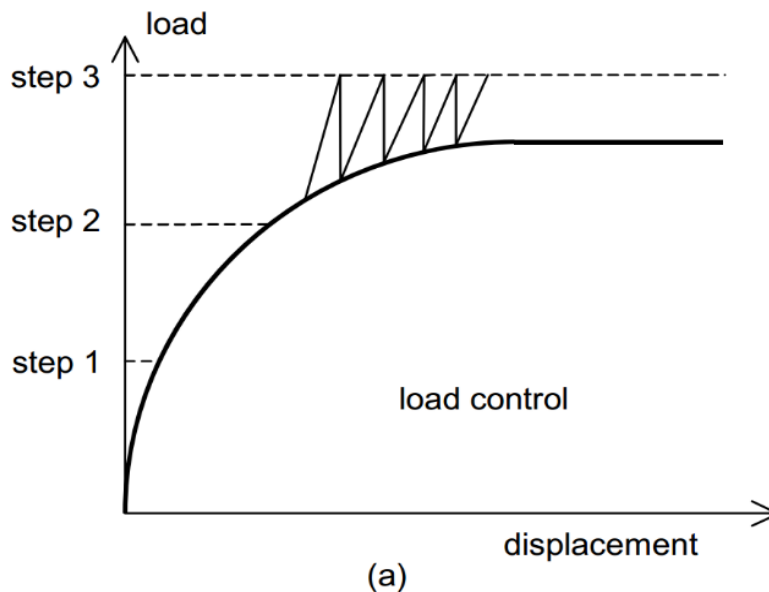


Figure 3.1 Iterative procedure for normal load control (Guler et al. ,2012)

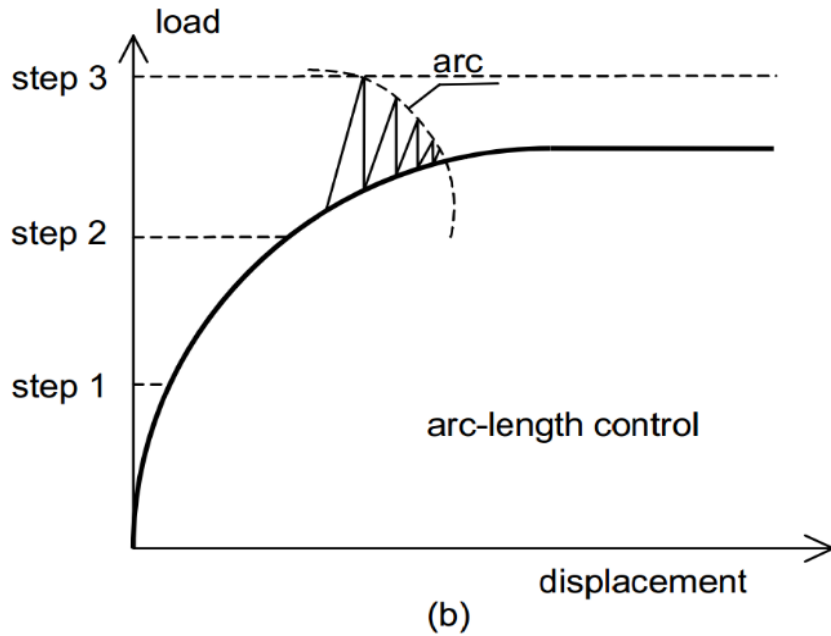


Figure 3.2 Iterative procedure for arc load control (Guler et al. ,2012)

3.2 GEOGRIDS

Geogrids are geosynthetic materials that are used to reinforce soils as well as other materials. Soils split under stress. In comparison to soil, geocell have a high tension. This allows them to spread pressures over a larger area of soil than is possible. Popular thermoplastics used in geogrids include polyester, polyvinyl alcohol, polythene, and polypropylene. They're manufactured by weaving or weaving yarns, heat connecting strips of fabric, or drilling a grid of holes in iron sheet and extending them into the a grid.



Figure 3.3 Photo of geogrids



Figure 3.4 Photo of GRS extensible reinforcement (geogrids)

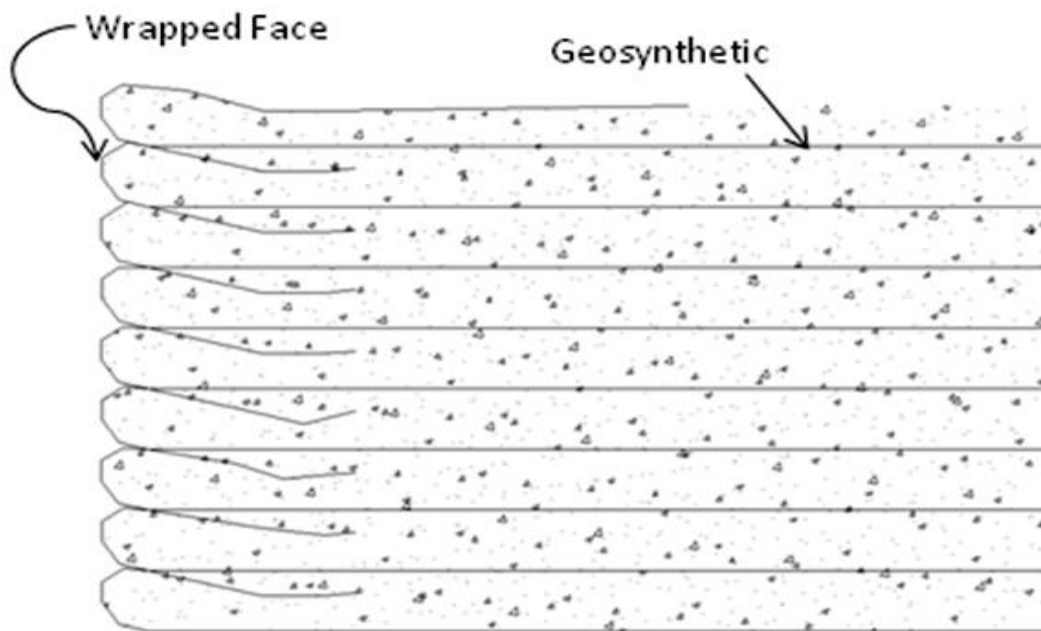


Figure 3.5 Typical wrapped face structure of GRS

Geogrids are utilised in the construction of retaining walls in soil backfills. The building of a solid retaining wall will be aided by holding the soil together. Geocells can be used to improve the structural stability of the soil. This facilitates in the distribution of loads as well as the confinement of backfill. Geogrids are utilised to solve problems like sloping ground and soft backfill.

CHAPTER – 4 METHODOLOGY

Philippe et al. (2016) performed the probabilistic analysis of the Reinforced Soil Wall to check the deformation and safety. Structural stability is modeled as a series of configuration and as r-out-of-m configuration. Redundancy of structure is formulated based on transitional probabilities. Failure propagates the different layer of reinforcement in the soil structure.

CONCEPT MODEL

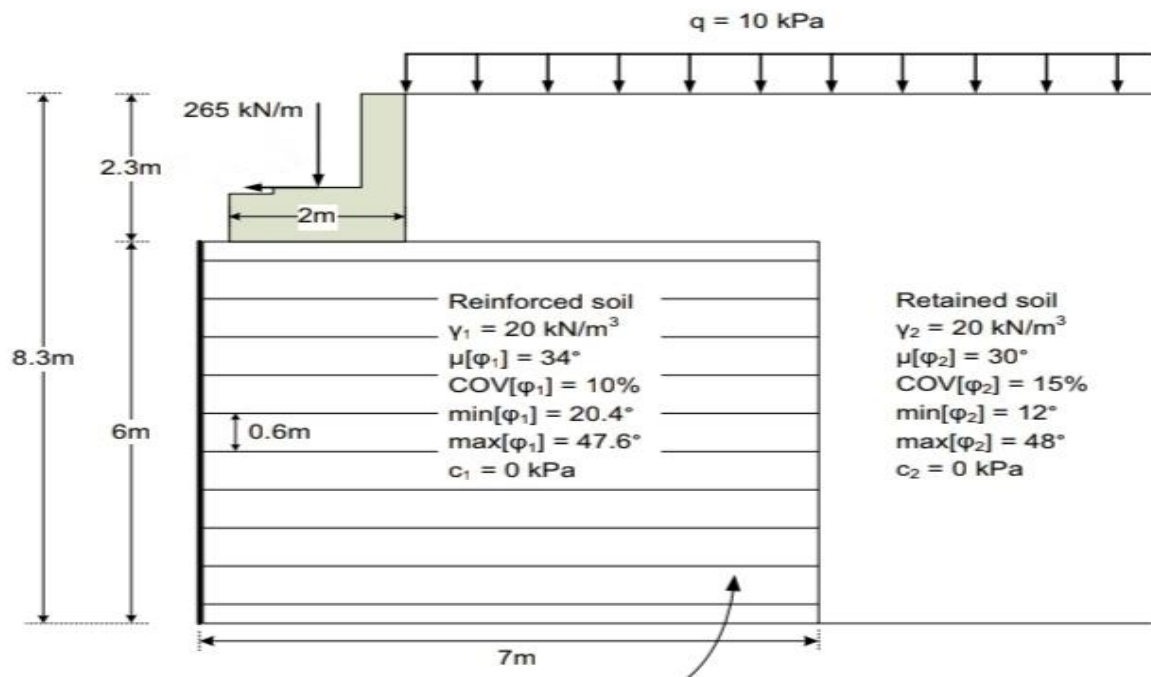


Figure 4.1 Model used for probabilistic analysis (Philippe et al. ,2016)

In this study, Concept model is analysed by commercially available software PLAXIS 2D. Same properties of backfill soil and geogrids are used to perform the simulation. Various load is applied, different curves are obtained from the simulation. Load transfer mechanism is shown by the Finite Element Analysis. This study mainly based on the behavior of backfill soil after applying various load,

and to the change of the soil structure.

In probabilistic analysis, 6-meter height of lower wall, 2.3 meter and 2-meter width of abutment has constructed over it. A surcharge of load 10kpa and point load (bridge load) 265kpa is applied over it.

In present study same parameters are used in PLAXIS 2D for the analysis, a series of surcharge load 5kpa, 10kpa, 15kpa, 20kpa and same point load 265kpa is applied. Deformation and safety analysis has performed.

MODEL FOR STUDY IN PLAXIS 2D

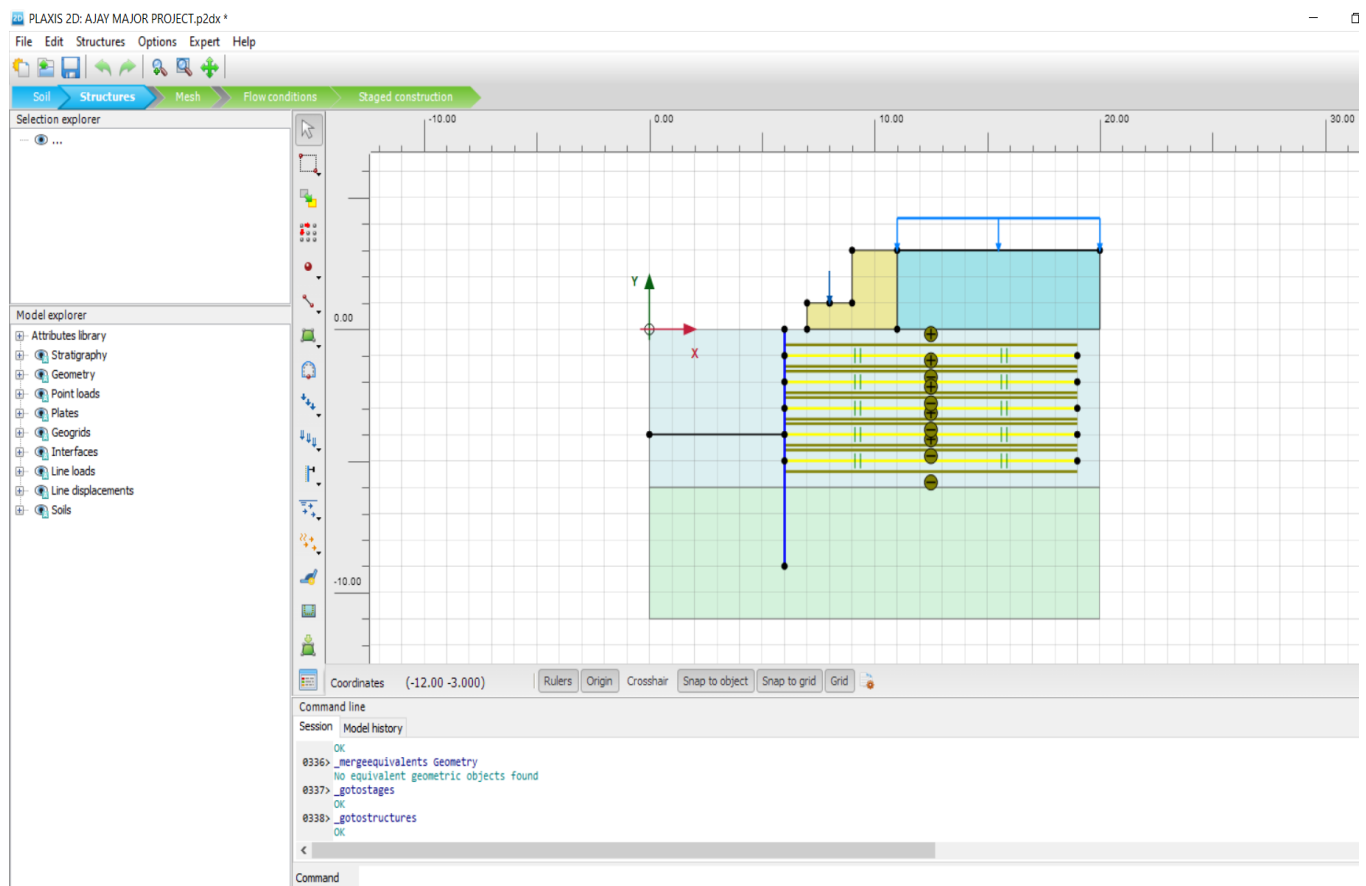


Figure 4.2 Model used in PLAXIS 2D for analysis

Table 4.1: Input parameters used in modeling, (Philippe et al, 2016)

Parameters	Backfill soil
Model	Mohr-Coulomb
Soil unit weight, γ (kN/m ³)	20
Modulus of elasticity E, (kN/m ²)	30,000
Poisson ratio (μ)	0.3
Cohesion (c)	0
Angle of internal friction ϕ , (degree)	34

Table 4.2: Properties of reinforcement used in modeling, (Philippe et al, 2016)

Length of reinforcement (m)	7
Spacing between reinforcement (m)	0.6
Axial stiffness (kN/m)	700

Table 4.3: Properties of concrete block in modelling, (mirmoradi et al. 2021)

Model	Linear elastic
Unit weight (kN/m ³)	22
Poisson ratio	0.15
Cohesion C, (kpa)	46
Angle of internal friction (degree)	57
Modulus of elasticity (E), (kN/m ²)	65,000

4.1 PHASE CONSTRUCTION IN PLAXIS 2D

The procedure of Lower GRS wall in PLAXIS 2D is defined in various phase. The data of wall has been collected in different phase,

Phase 1: Lower GRS wall of height 6m is constructed.

Phase 2: A 2.3m height abutment is constructed over the Lower GRS wall.

Phase 3: Geogrids and backfill soil placed in the Lower GRS wall.

Phase 4: Various Surcharge loading is applied over it.

Phase 5: A fix point load is applied on the abutment.

Phase 6: Calculate the deformation and factor of safety for soil structure

CHAPTER 5 – RESULTS AND DISCUSSION

5.1 DEFORMATION ANALYSIS IN PLAXIS 2D

5.1.1 Surcharge load = 5kpa, Bridge load (point load) = 265kpa

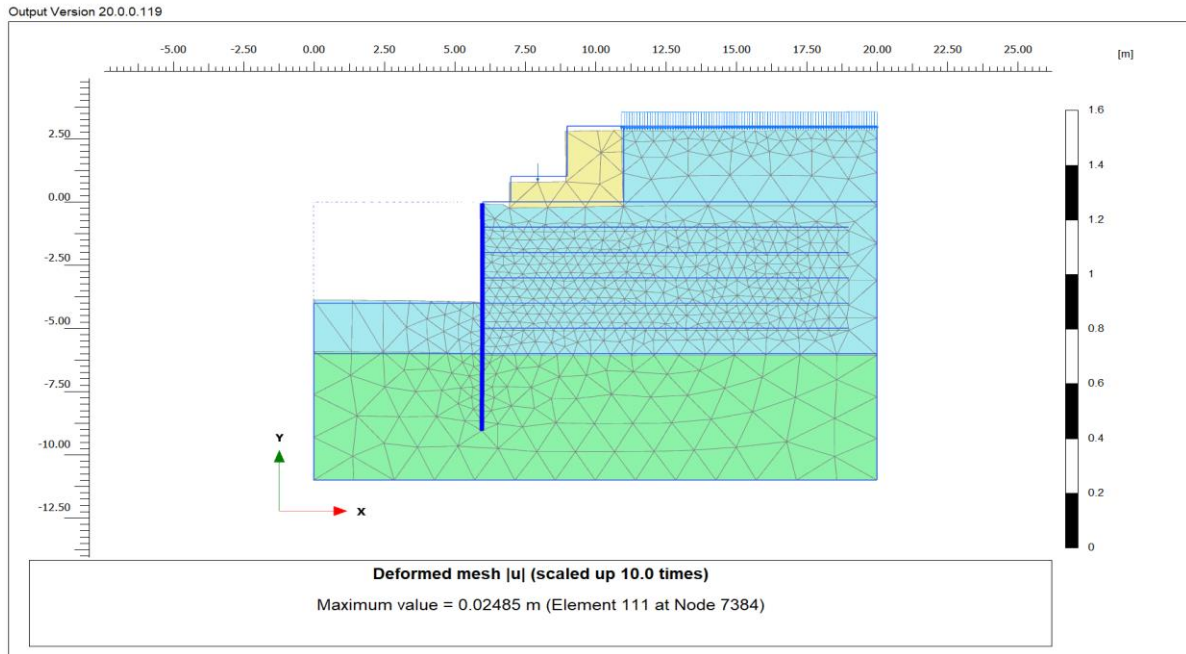


Figure 5.1: Deformation without geogrids

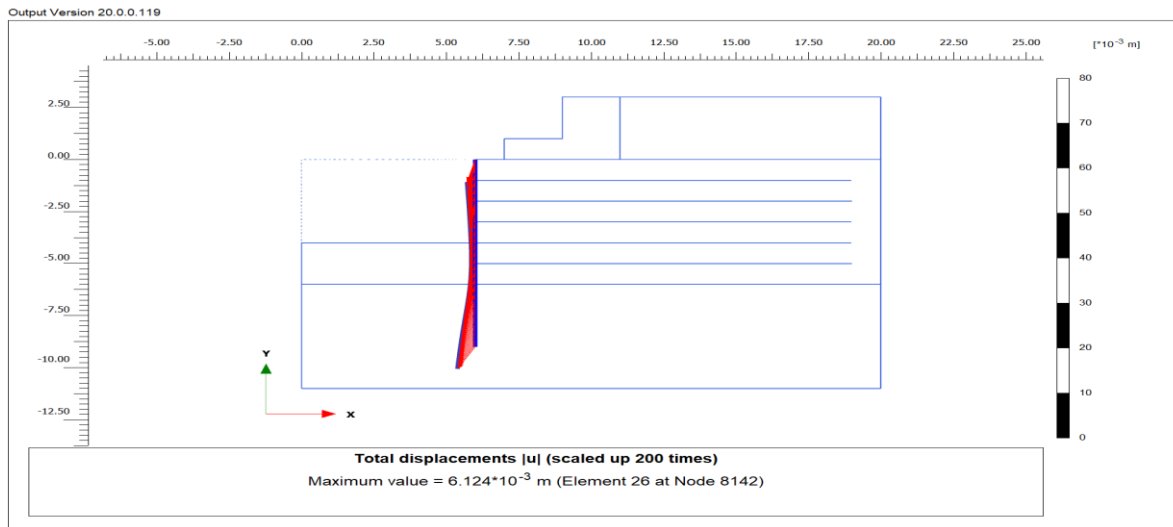


Figure 5.2: Wall displacement without geogrids

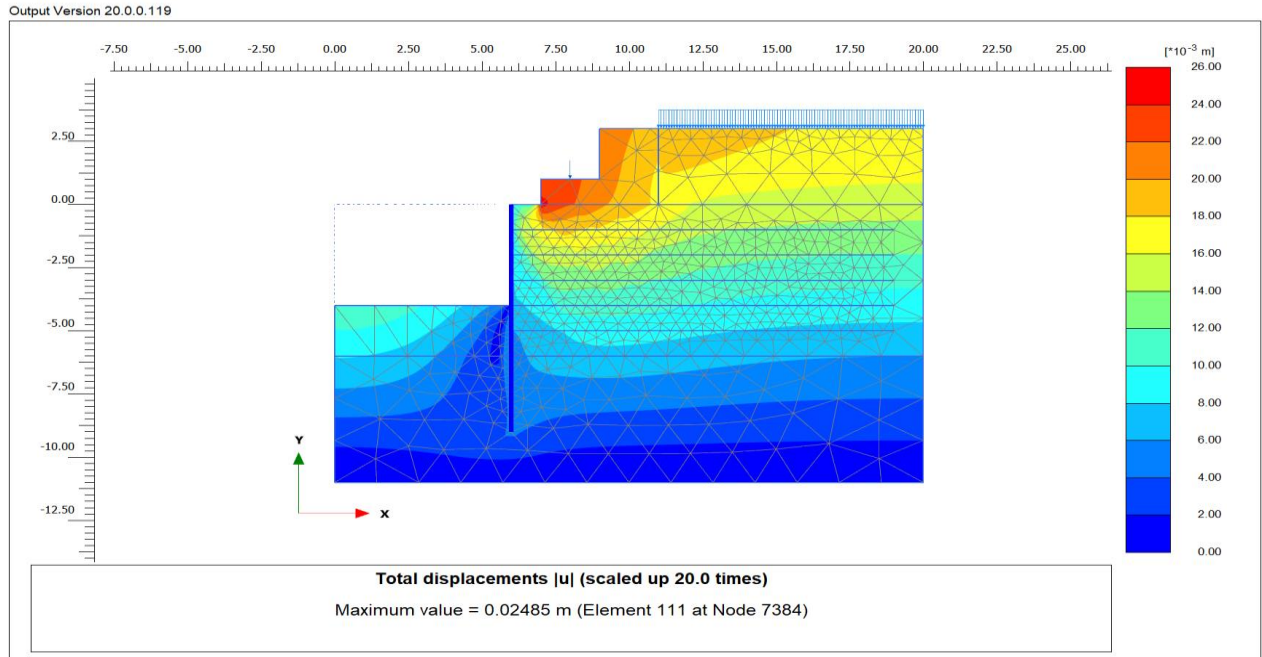


Figure 5.3: Deformed mesh of model without geogrids

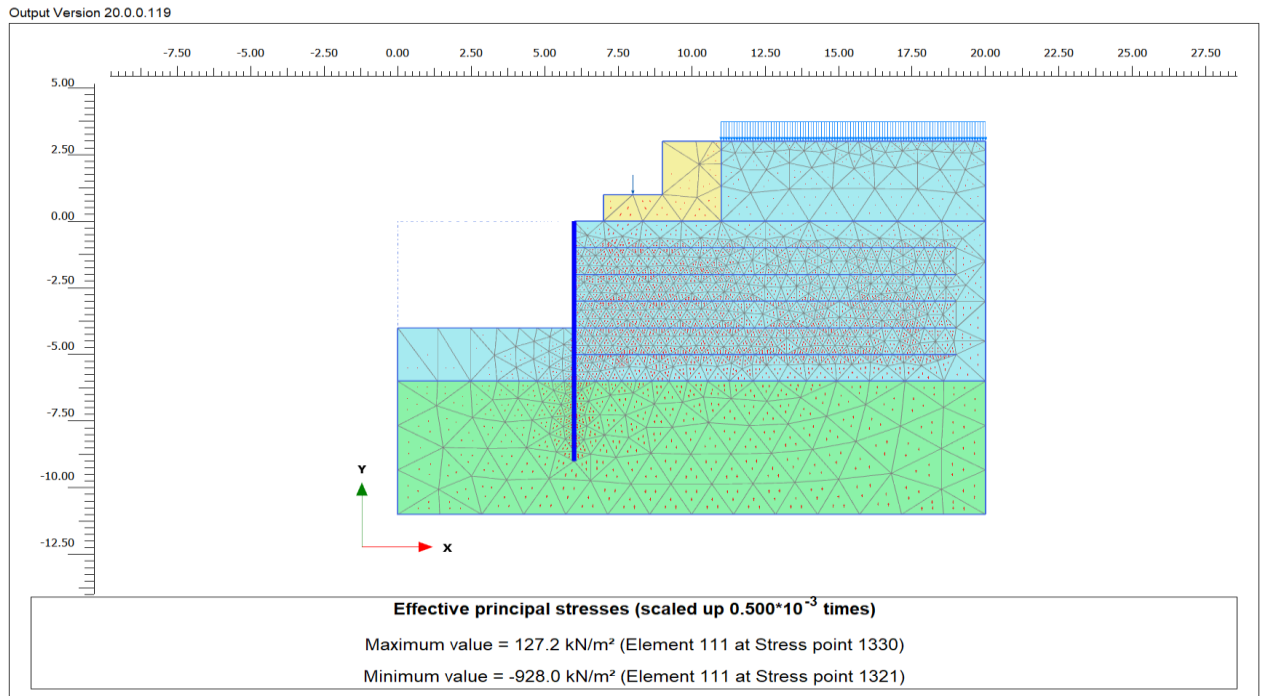


Figure 5.4: stresses mesh without geogrid

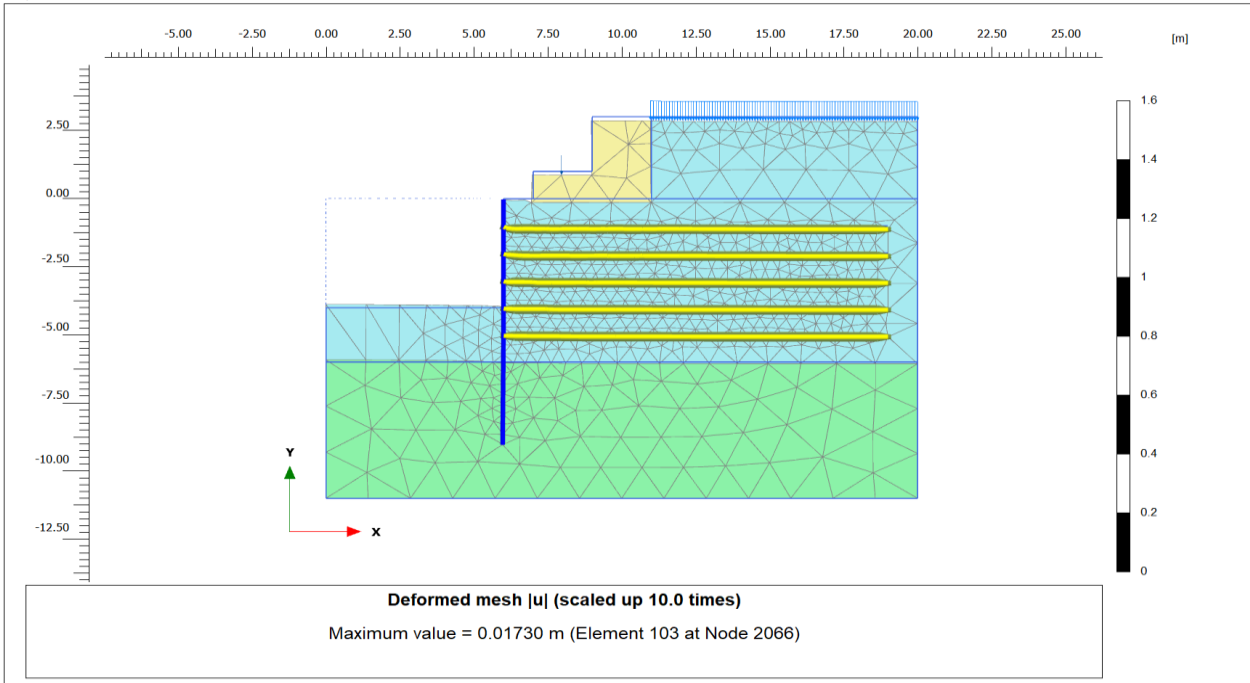


Figure 5.5: Deformation with geogrids

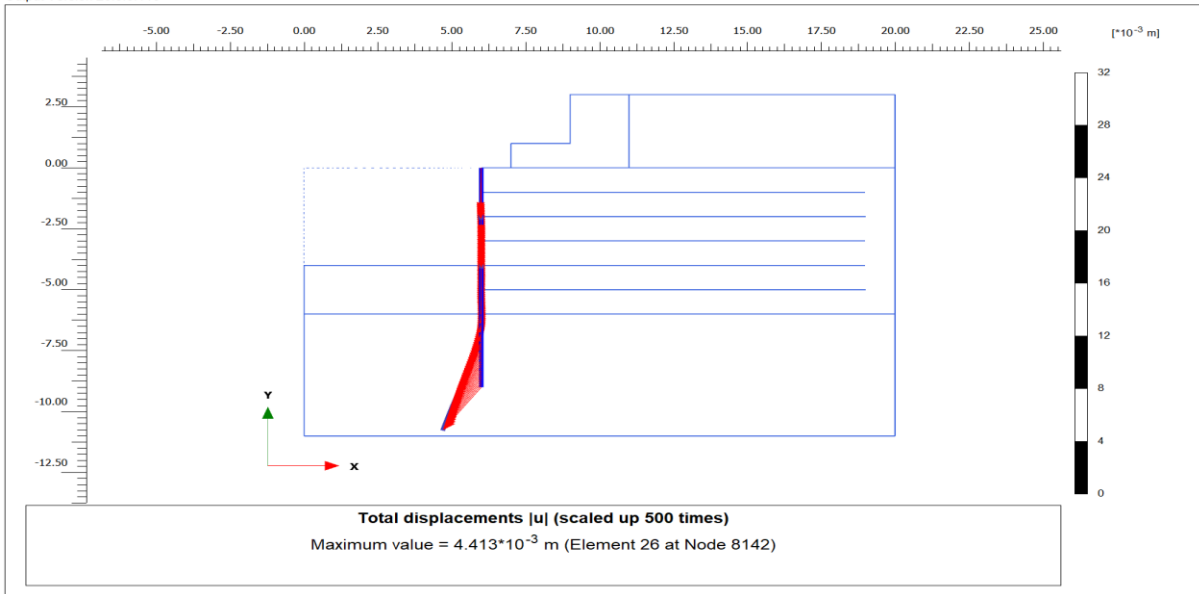


Figure 5.6: Wall displacements with geogrids

Output Version 20.0.0.119

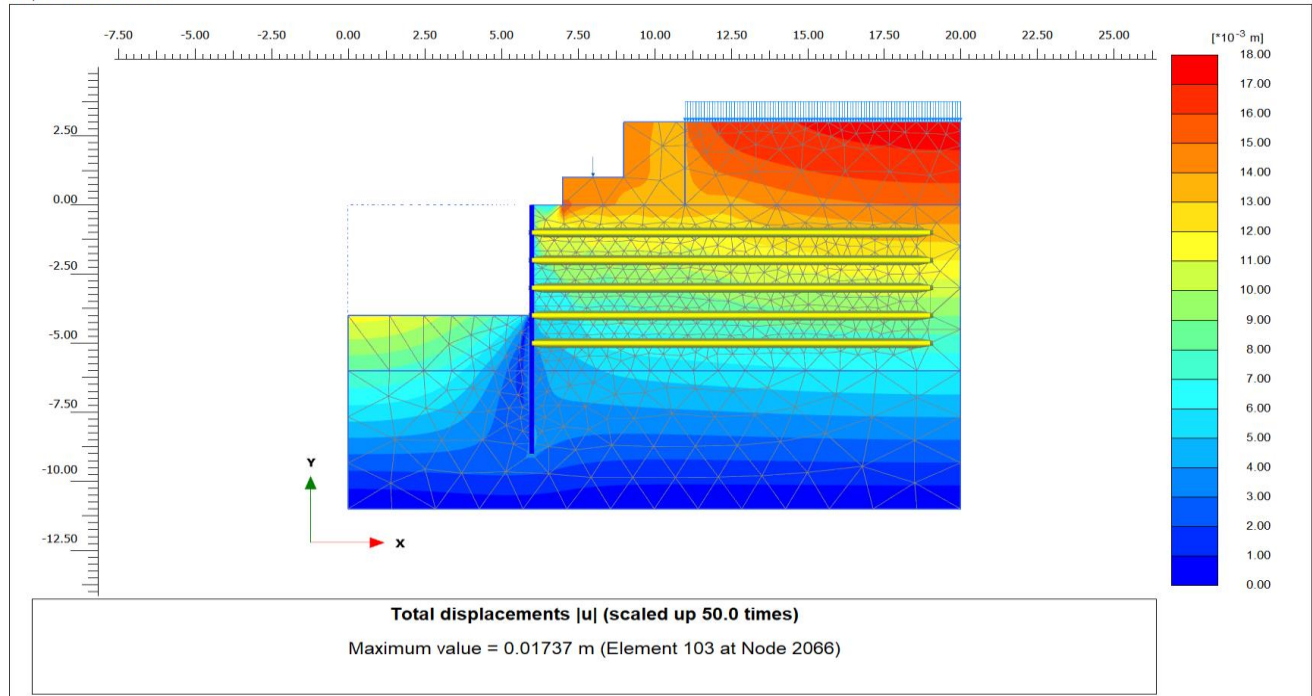


Figure 5.7: Deformed mesh of model with geogrids

Output Version 20.0.0.119

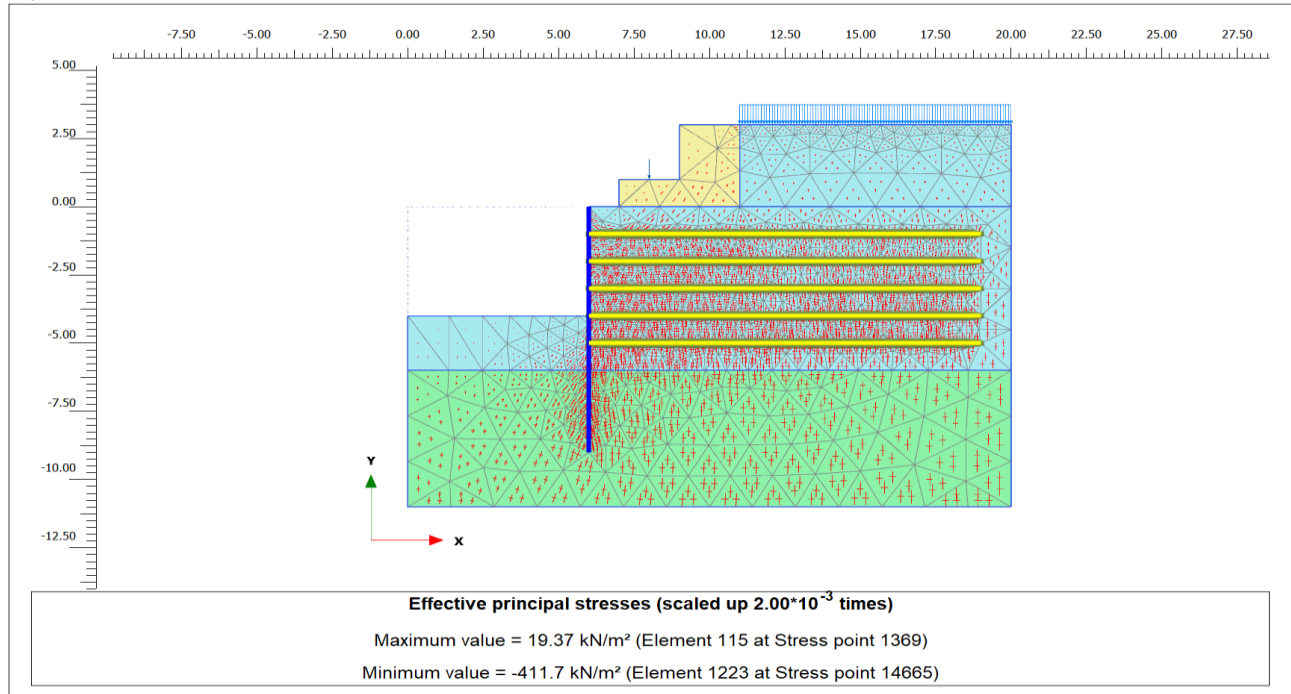


Figure 5.8: Stresses mesh with geogrids

5.1.2 Surcharge load = 10kpa, point load = 265kpa

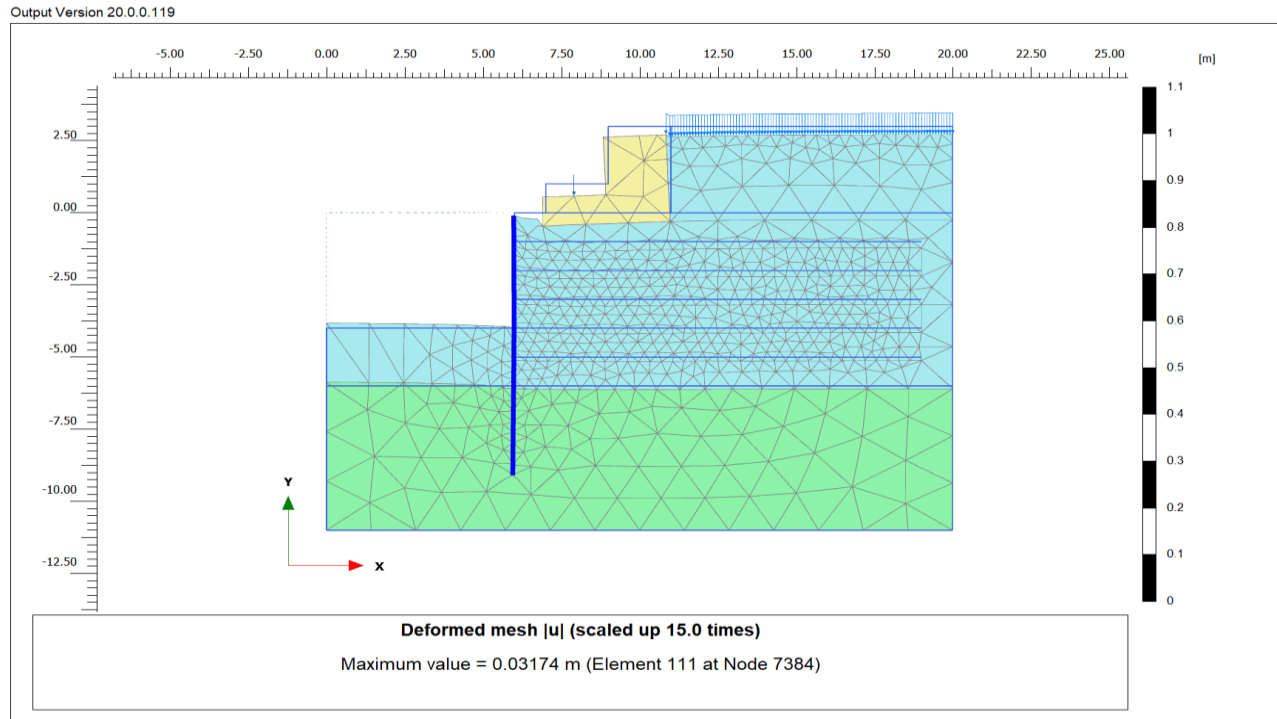


Figure 5.9: Deformation without geogrids

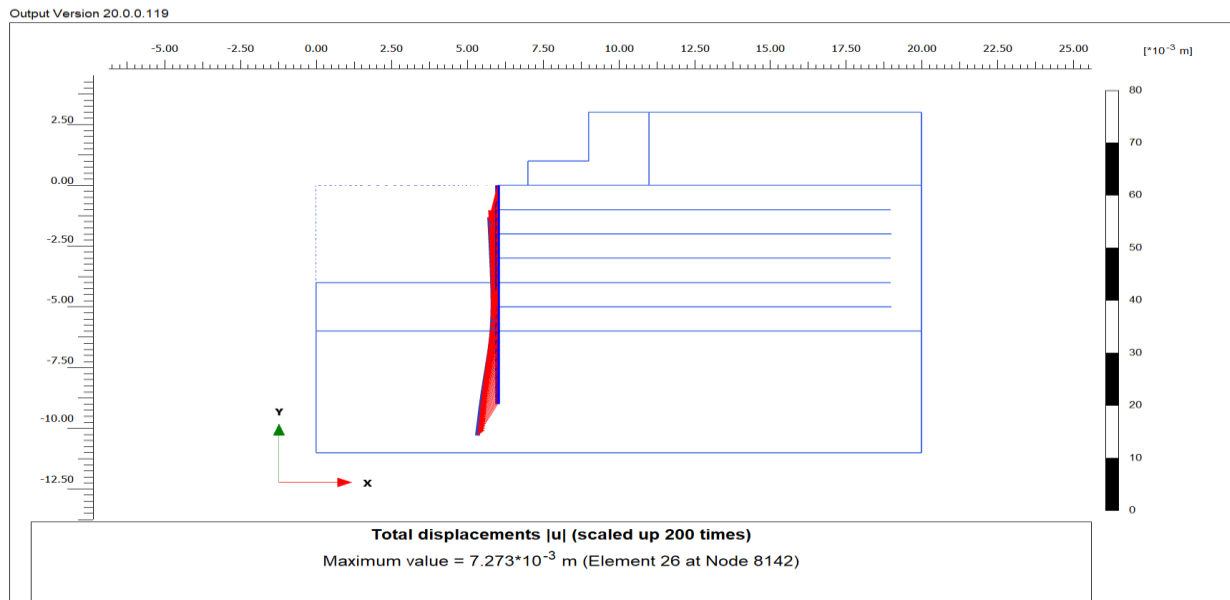


Figure 5.10: Wall displacement without geogrids

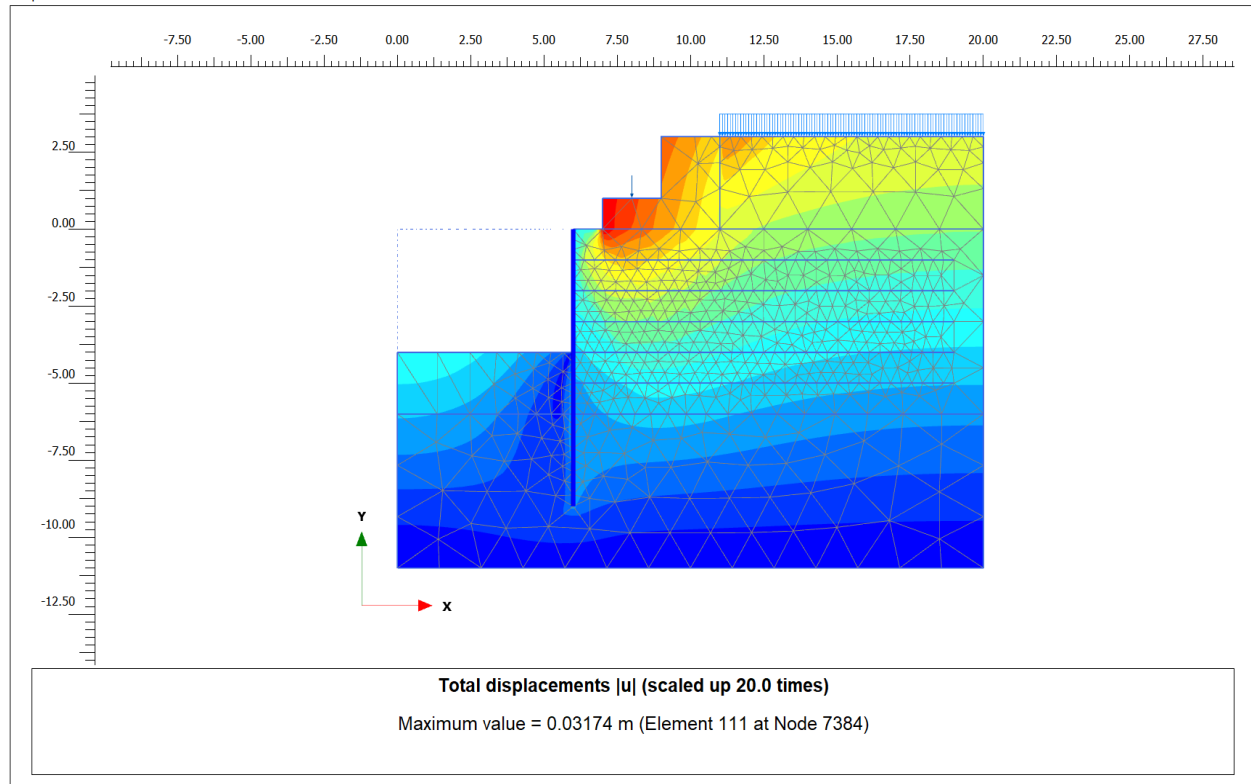


Figure 5.11: Deformation mesh of model without geogrids

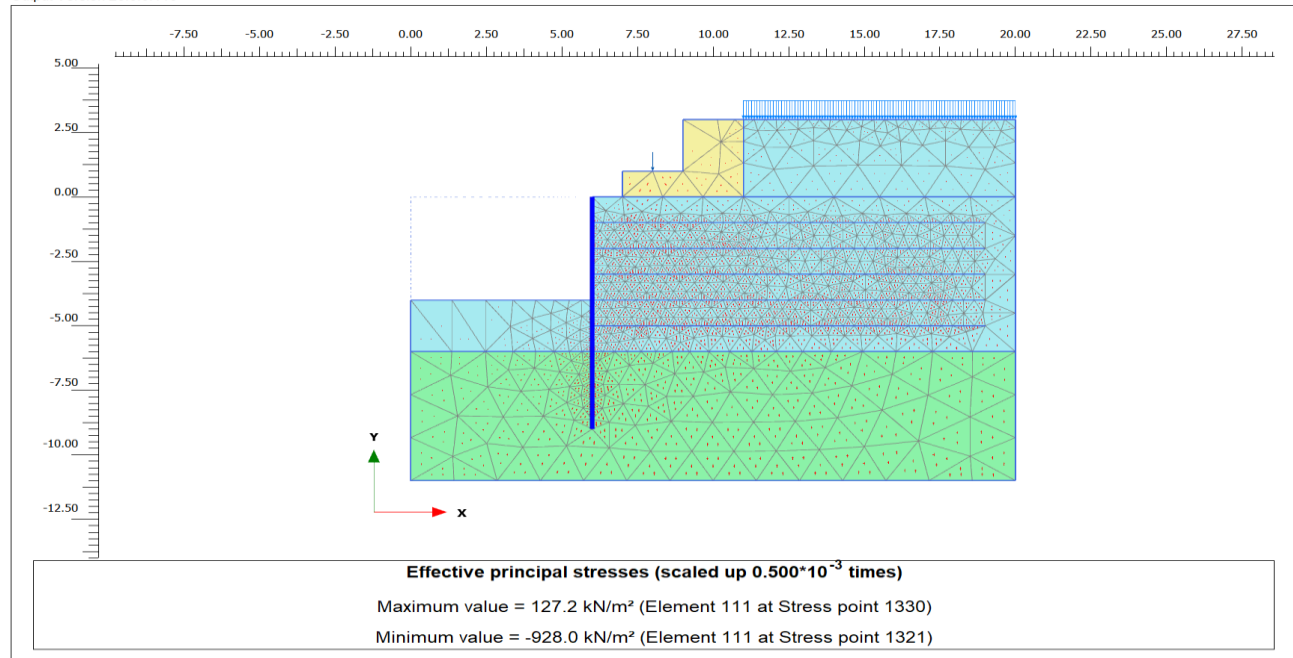


Figure 5.12: Stresses mesh without geogrid

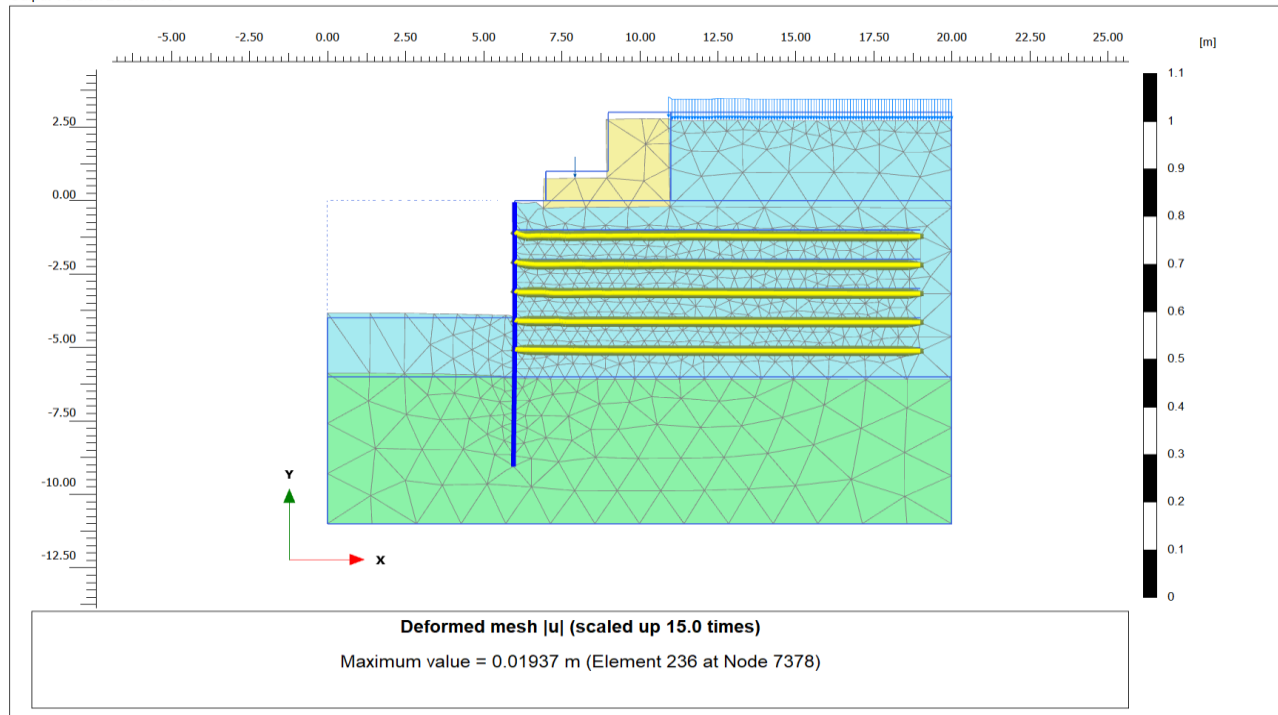


Figure 5.13: Deformation with geogrids

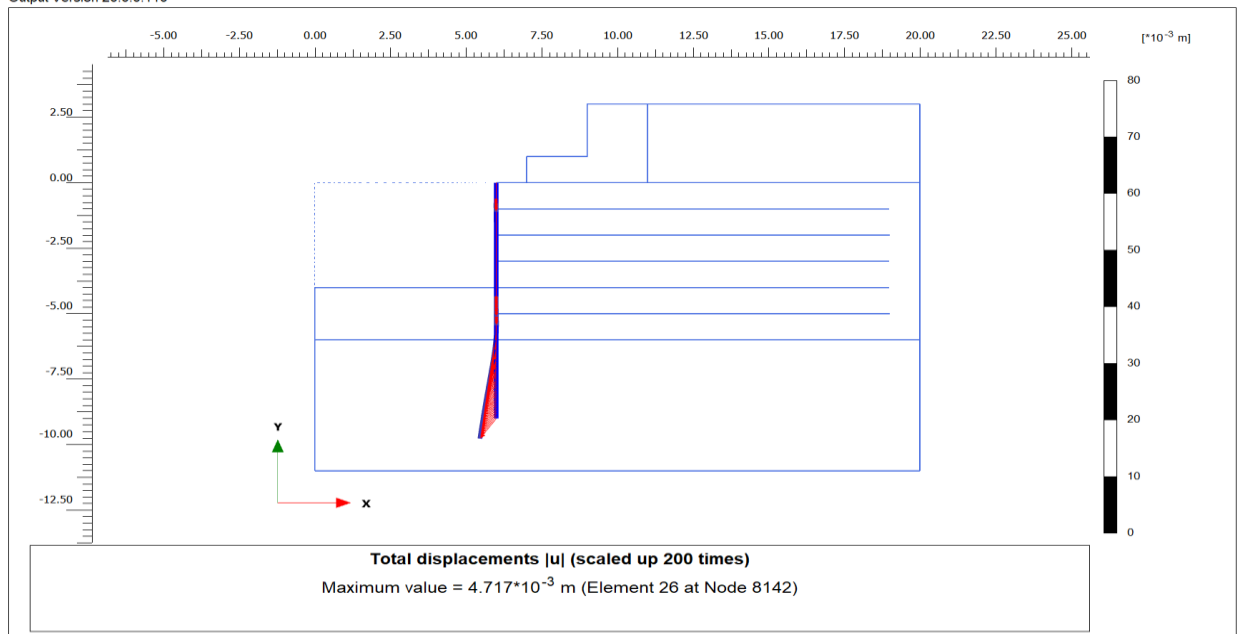
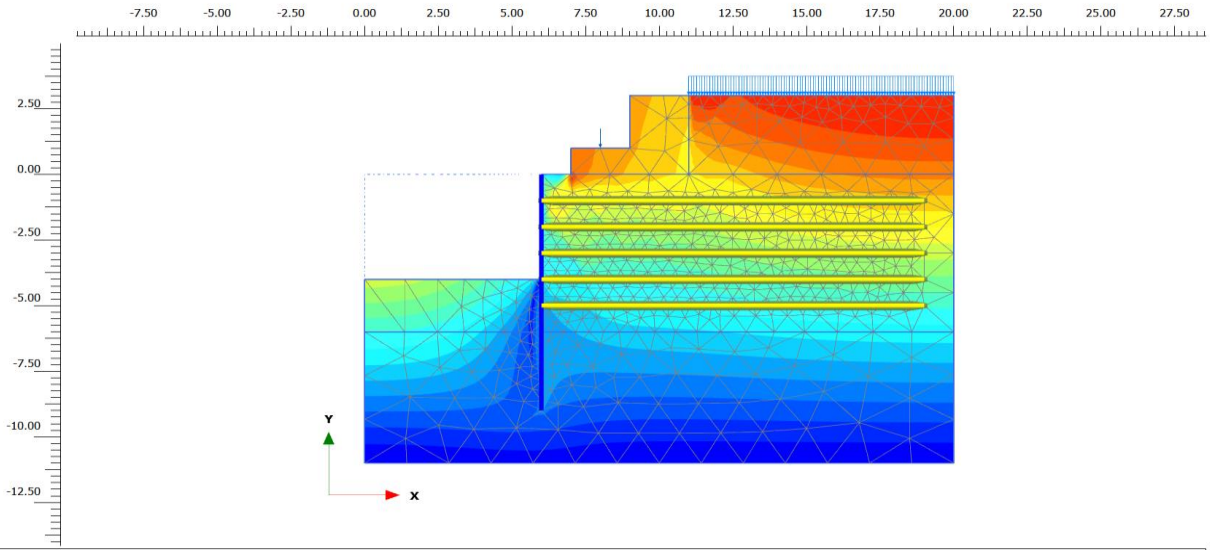


Figure 5.14: Wall displacement with geogrids

Output Version 20.0.0.119

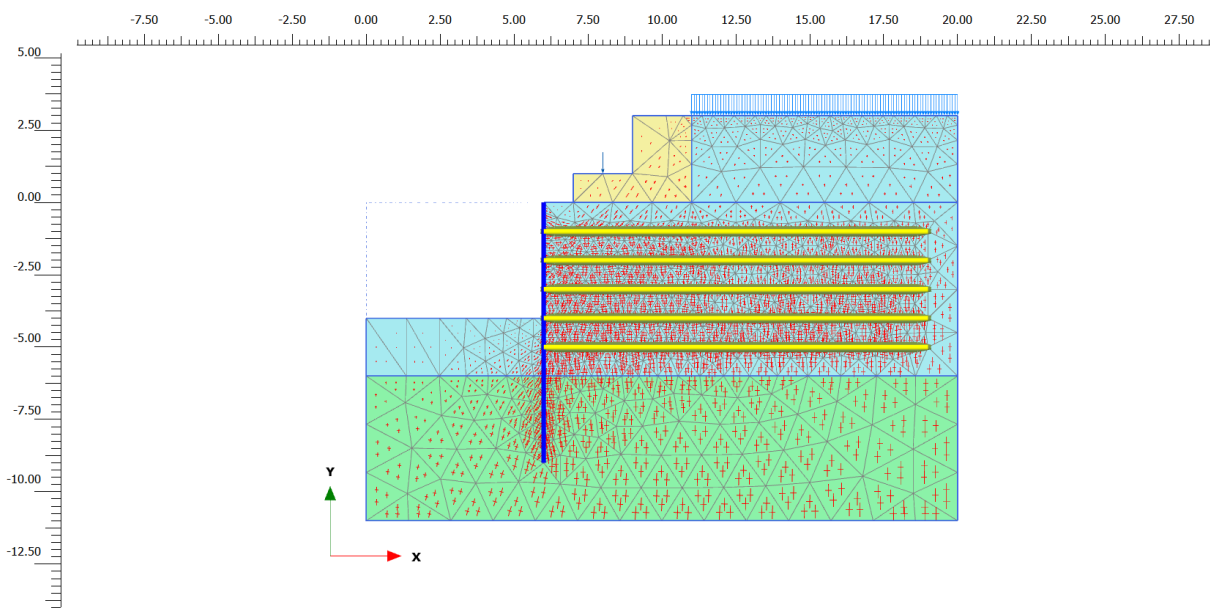


Total displacements |u| (scaled up 50.0 times)

Maximum value = 0.01899 m (Element 103 at Node 2066)

Figure 5.15: Deformation mesh of model with geogrids

Output Version 20.0.0.119



Effective principal stresses (scaled up $2.00 \cdot 10^{-3}$ times)

Maximum value = 19.37 kN/m² (Element 115 at Stress point 1369)

Minimum value = -411.7 kN/m² (Element 1223 at Stress point 14665)

Figure 5.16: Stresses mesh with geogrids

5.1.3 Surcharge load = 15kpa, point load = 265kpa

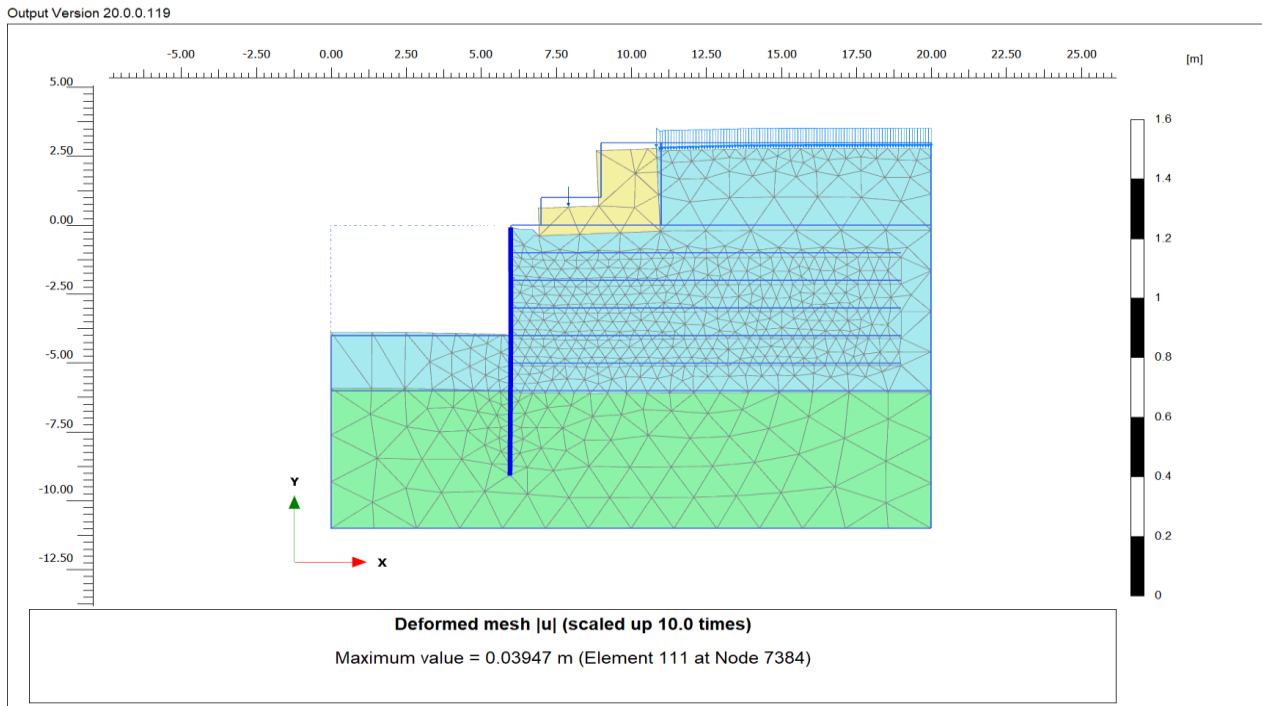


Figure 5.17: Deformation without geogrids

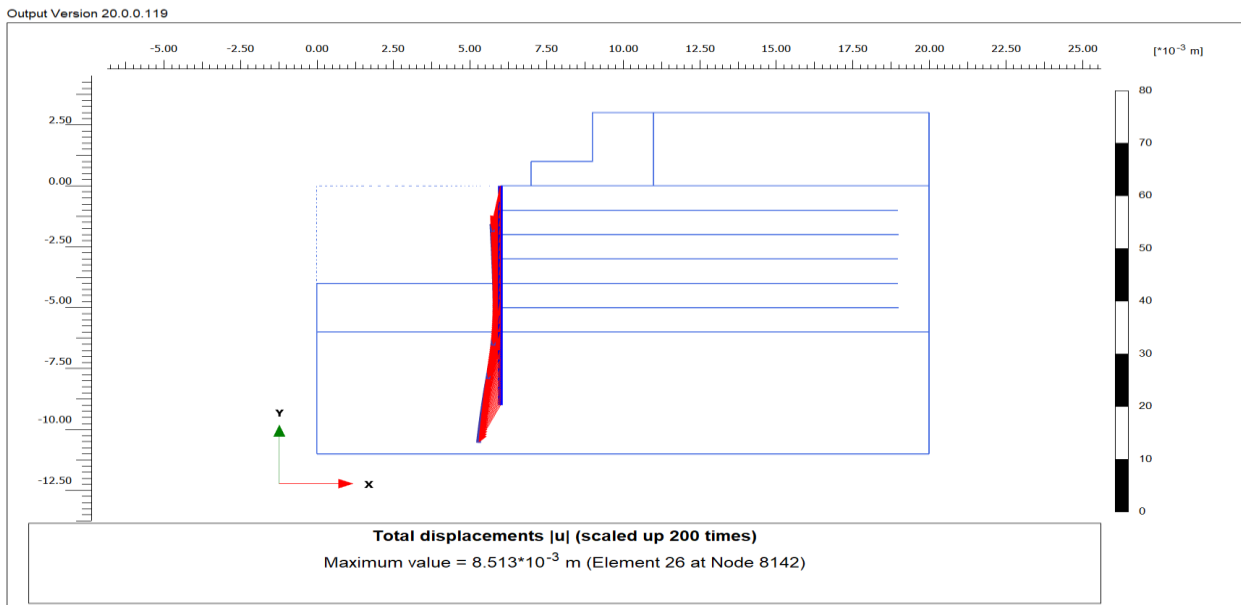


Figure 5.18: Wall displacement without geogrids

Output Version 20.0.0.119

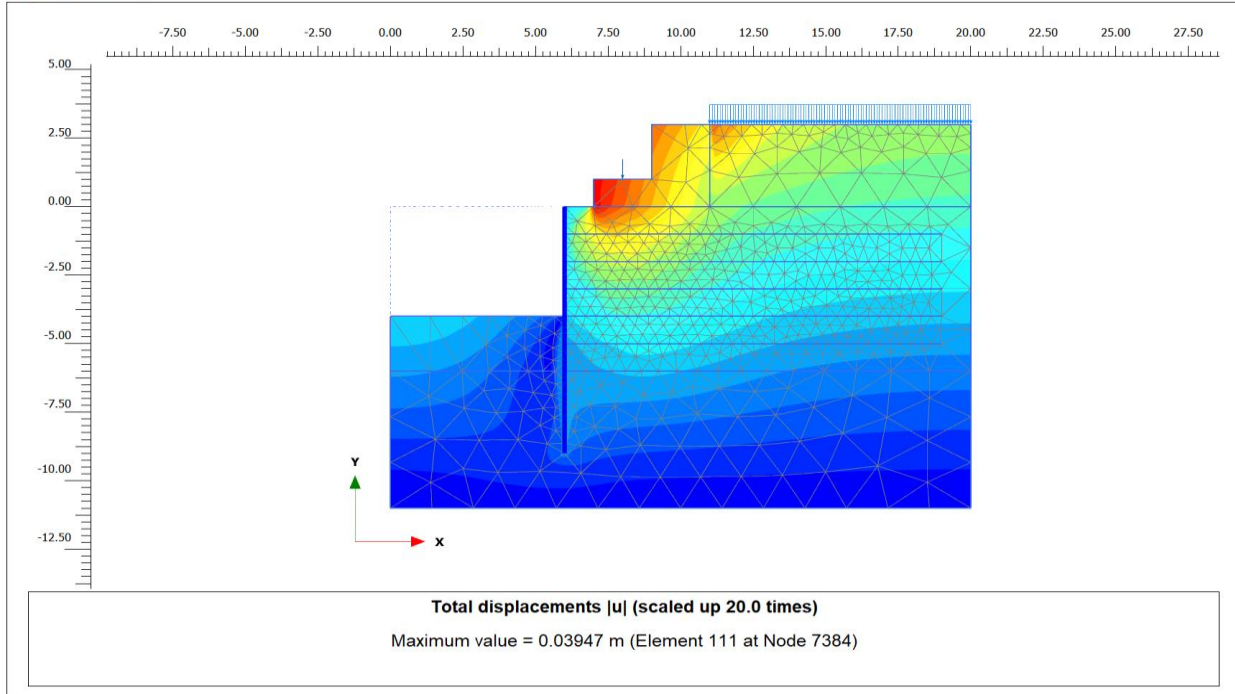


Figure 5.19: deformed mesh of model without geogrids

Output Version 20.0.0.119

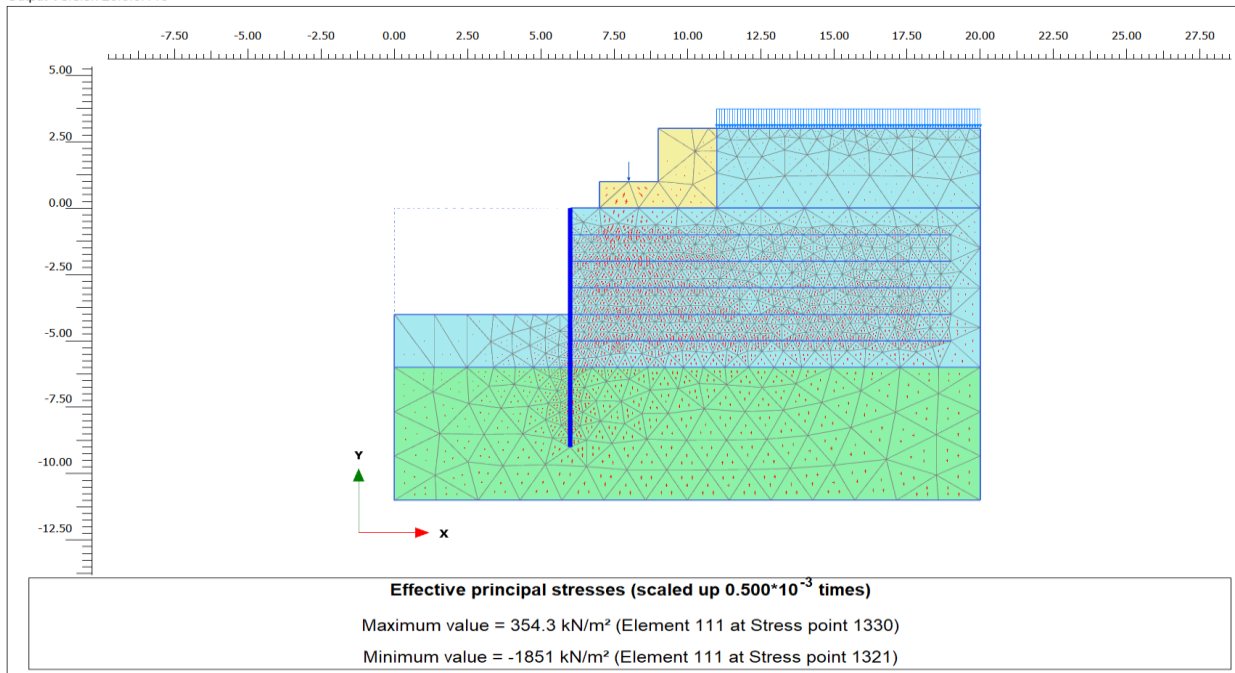


Figure 5.20: stresses mesh without geogrid

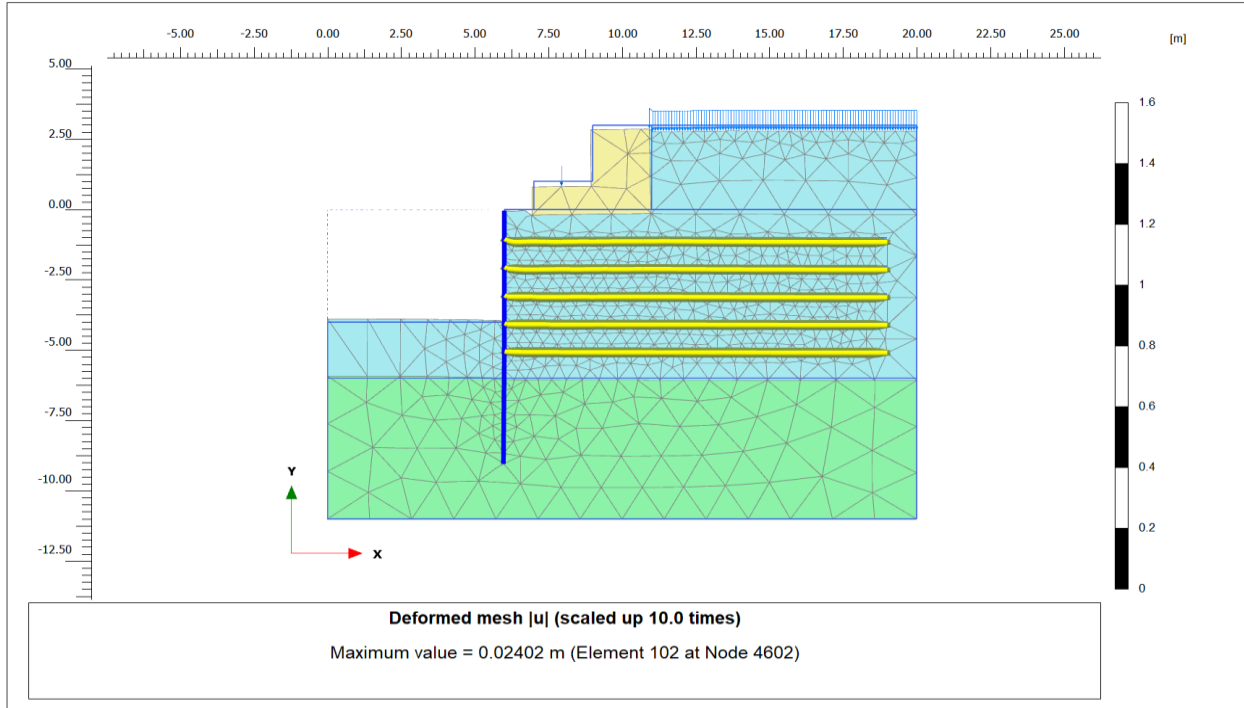


Figure 5.21: Deformation with geogrids

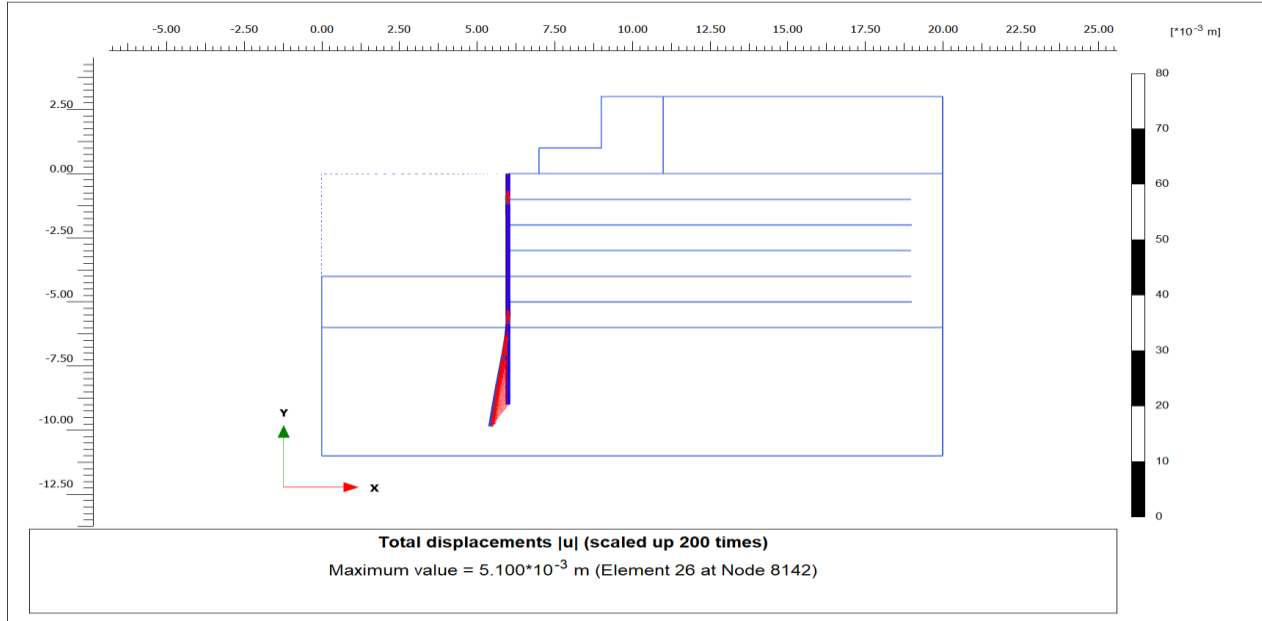


Figure 5.22: Wall displacement with geogrids

Output Version 20.0.0.119

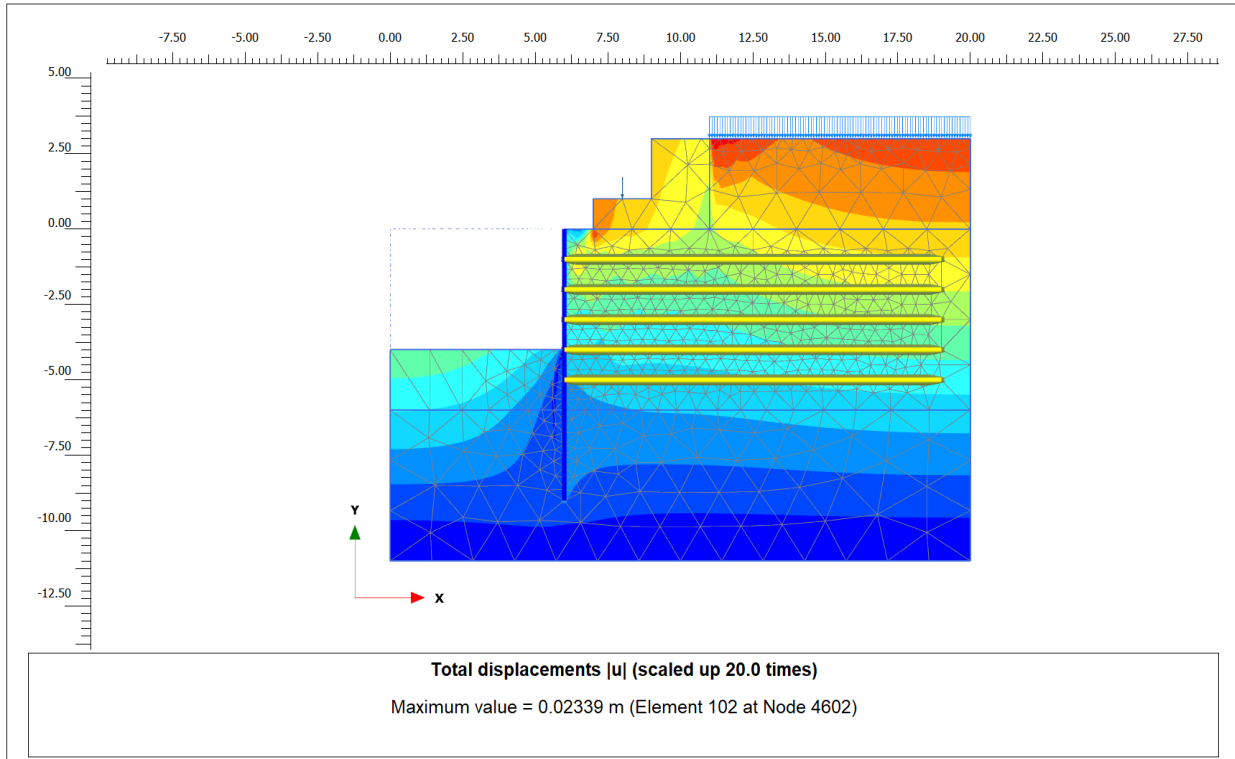


Figure 5.23: Deformed mesh of model with geogrids

Output Version 20.0.0.119

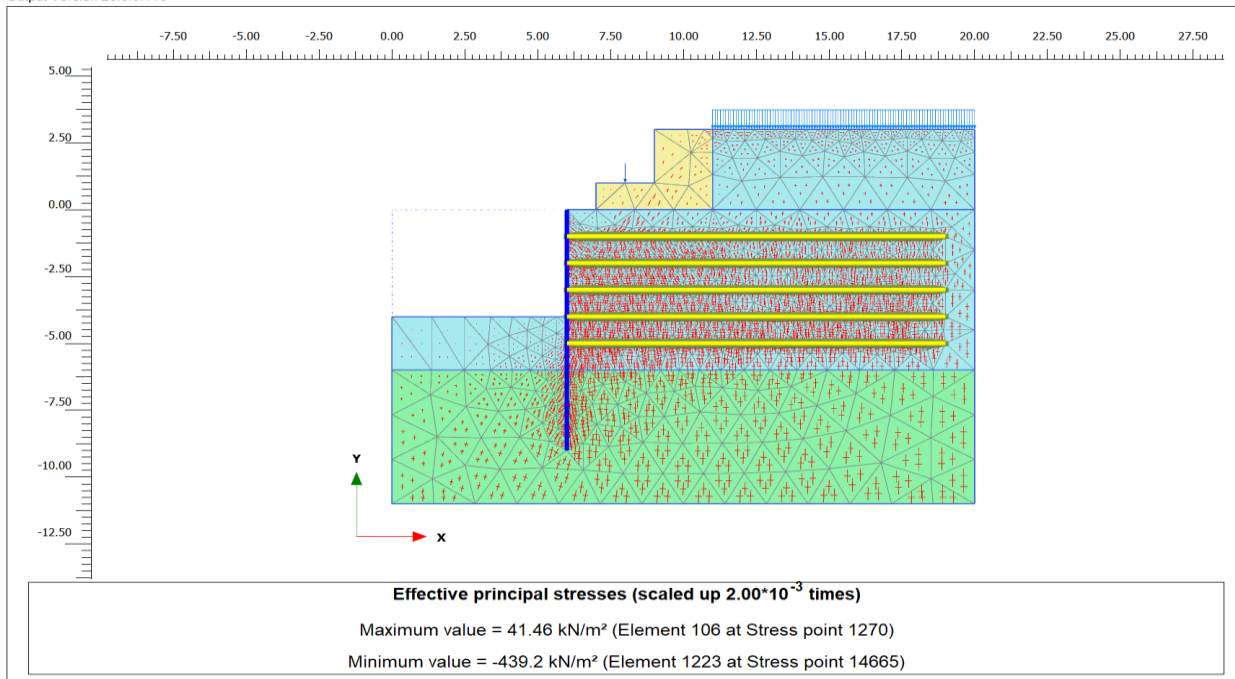


Figure 5.24: Stresses mesh with geogrid

5.1.4 Surcharge load = 20kpa, point load = 265kpa

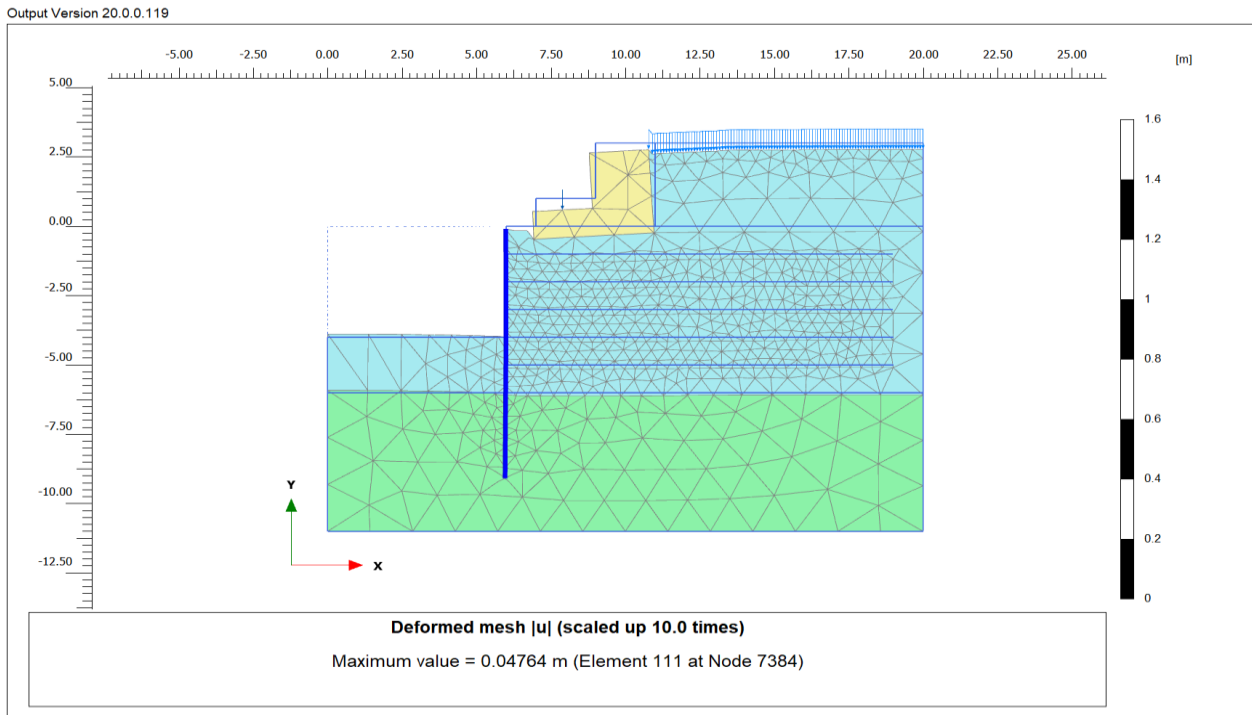


Figure 5.25: Deformation without geogrids

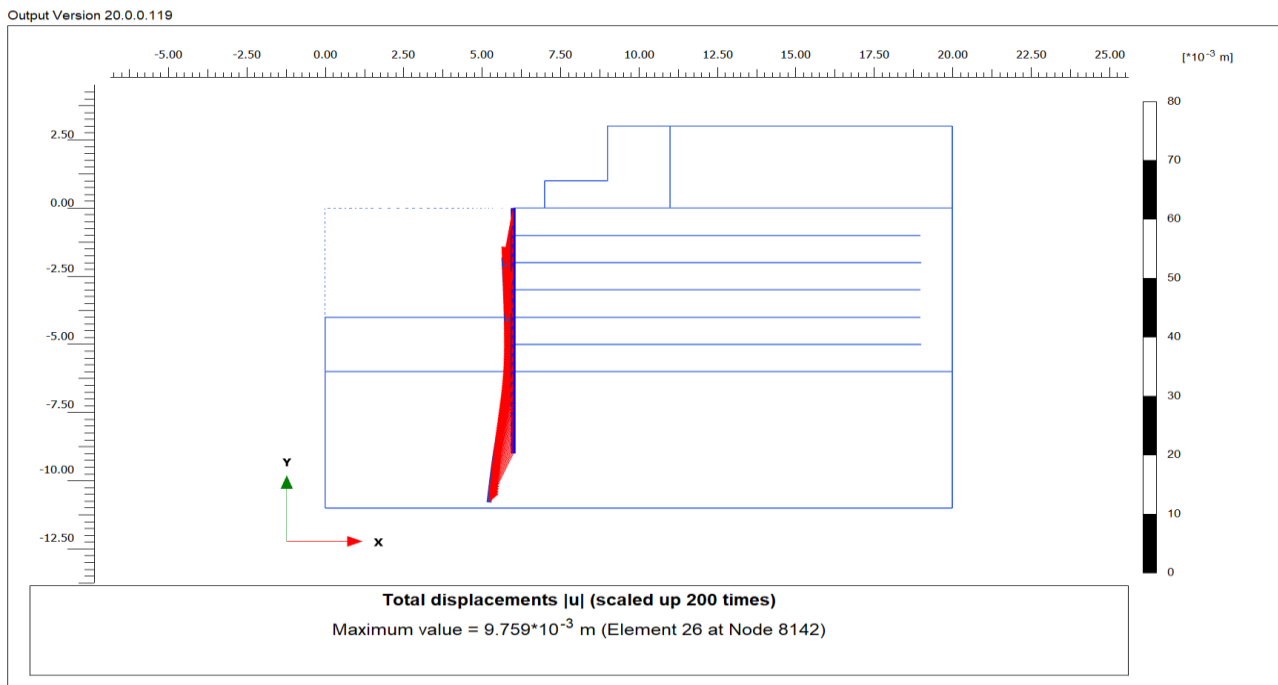


Figure 5.26: Displacement of wall without geogrids

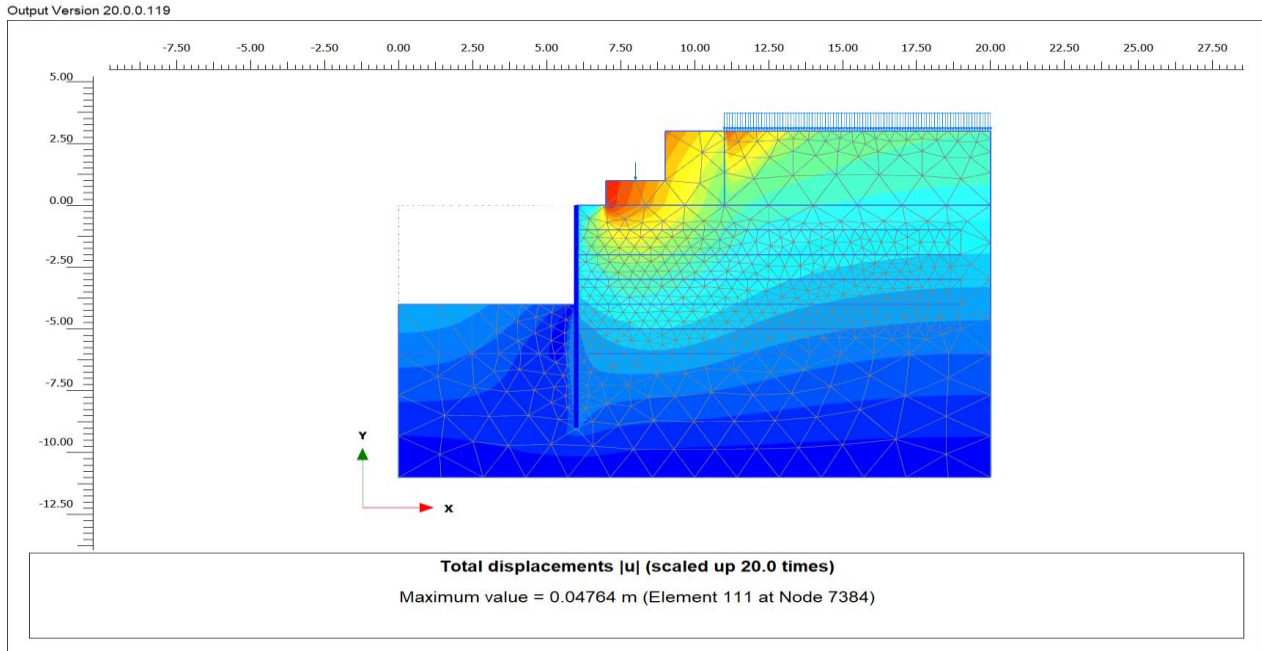


Figure 5.27: Deformed mesh of model without geogrids

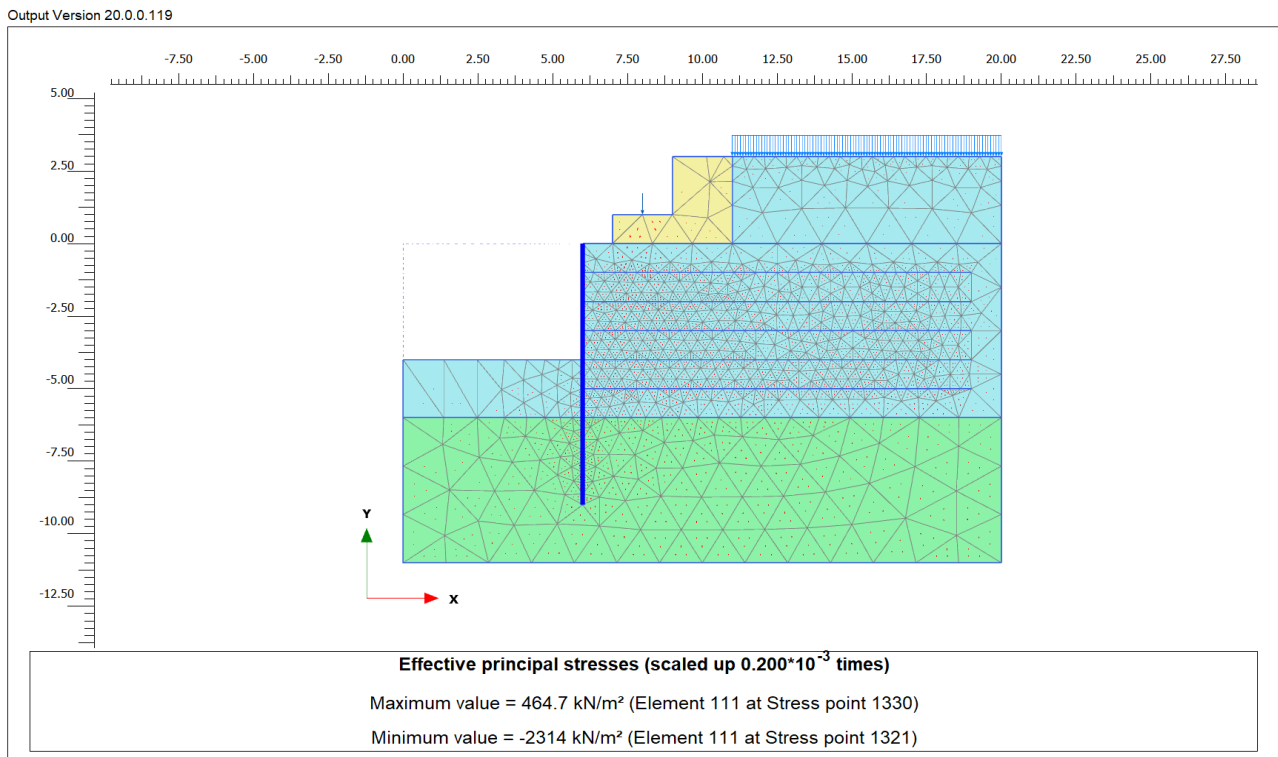


Figure 5.28: Stresses mesh without geogrids

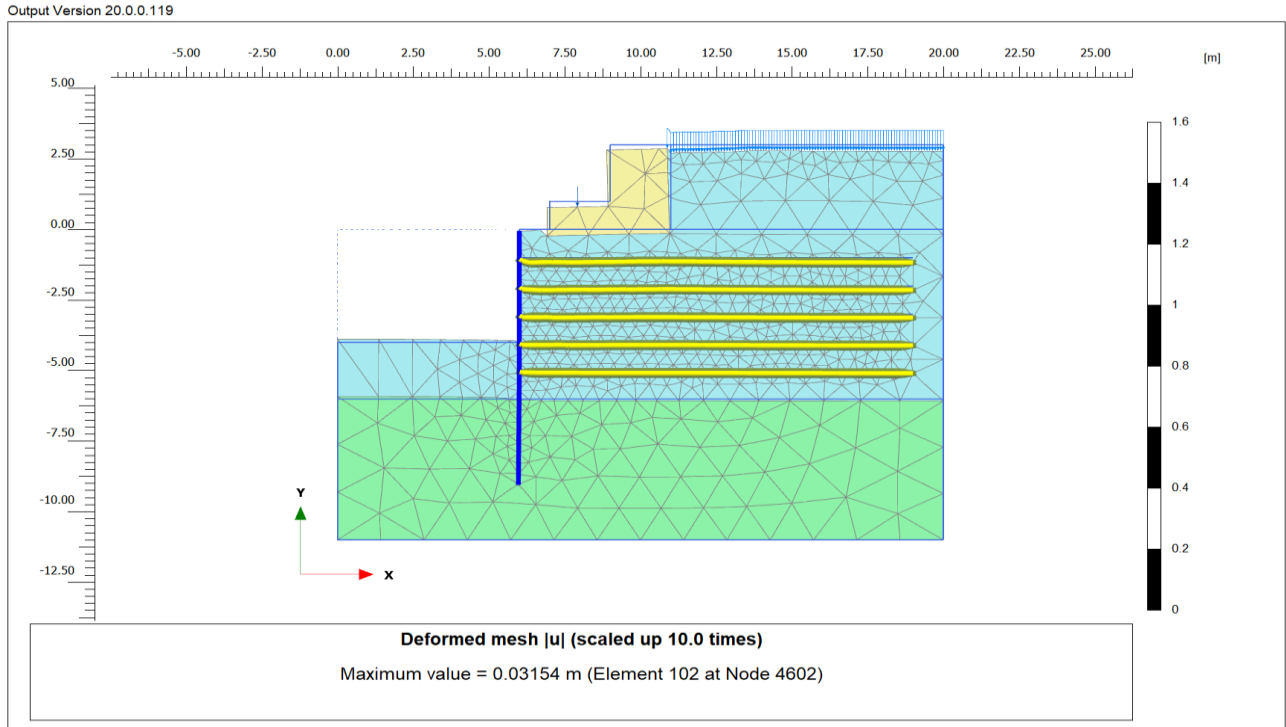


Figure 5.29: Deformation with geogrids

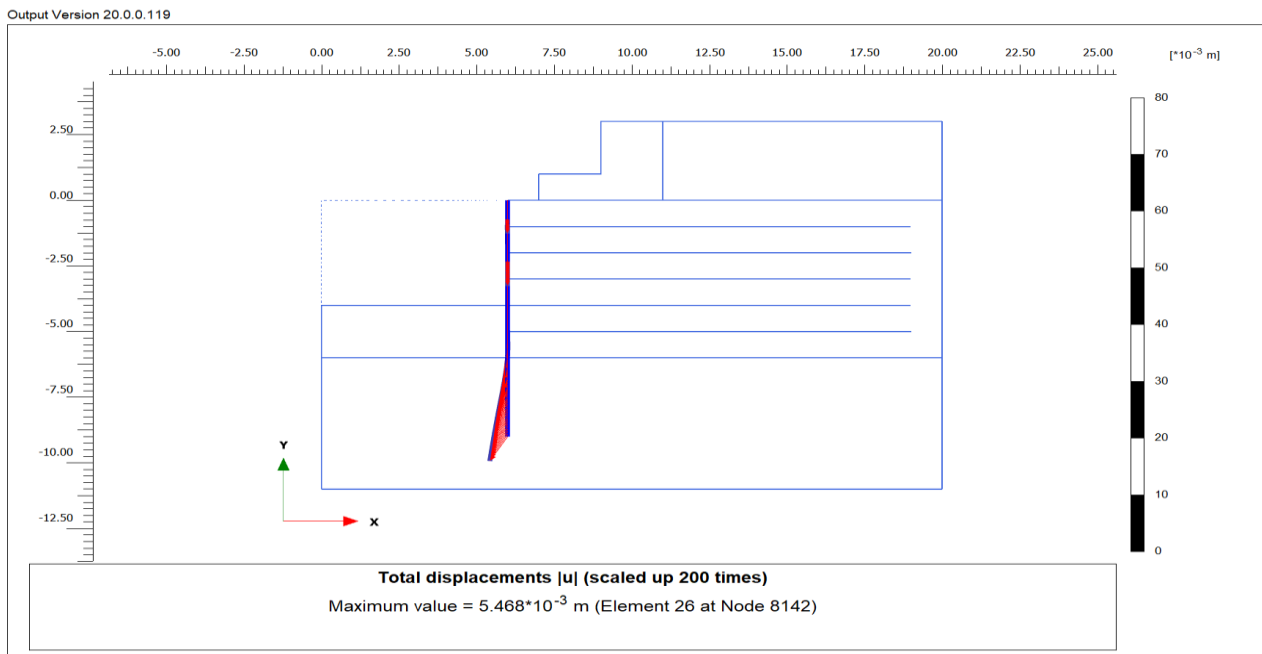
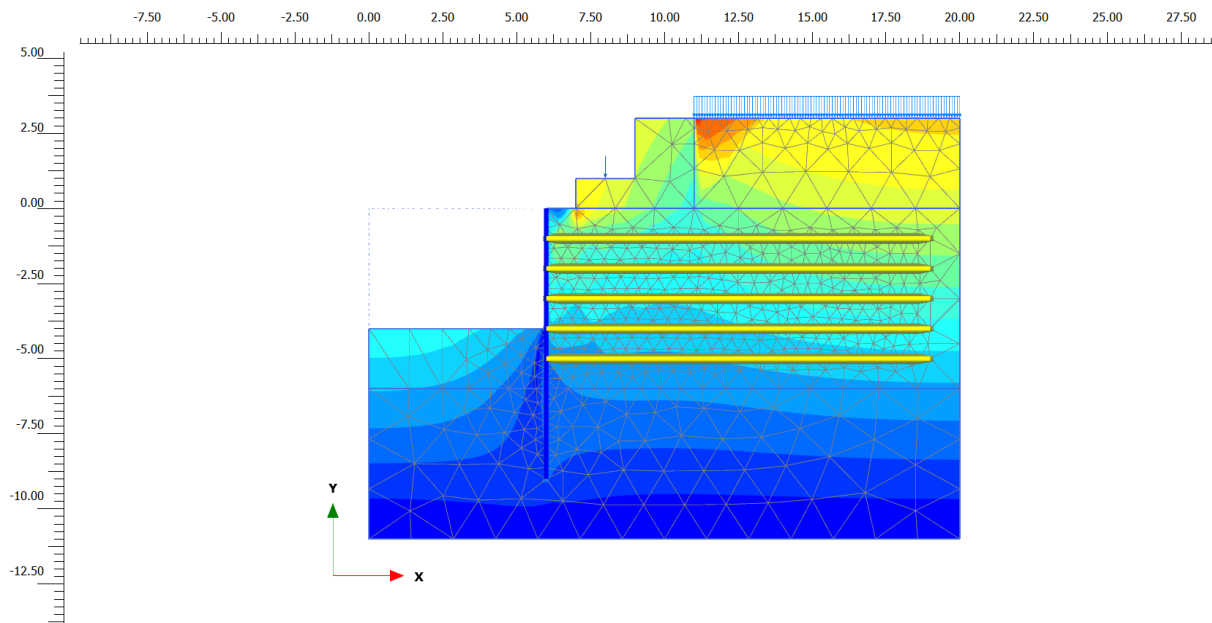


Figure 5.30: Wall displacements with geogrids

Output Version 20.0.0.119

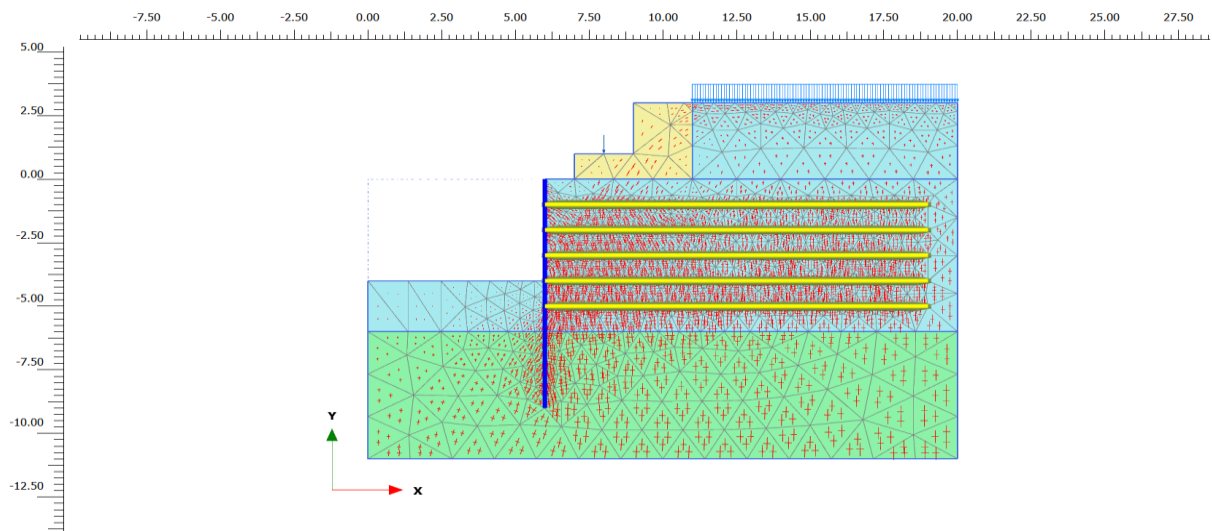


Total displacements |u| (scaled up 20.0 times)

Maximum value = 0.03074 m (Element 102 at Node 4602)

Figure 5.31: Deformed mesh of model with geogrids

Output Version 20.0.0.119



Effective principal stresses (scaled up $2.00 \cdot 10^{-3}$ times)

Maximum value = 44.28 kN/m² (Element 106 at Stress point 1270)

Minimum value = -444.8 kN/m² (Element 1223 at Stress point 14665)

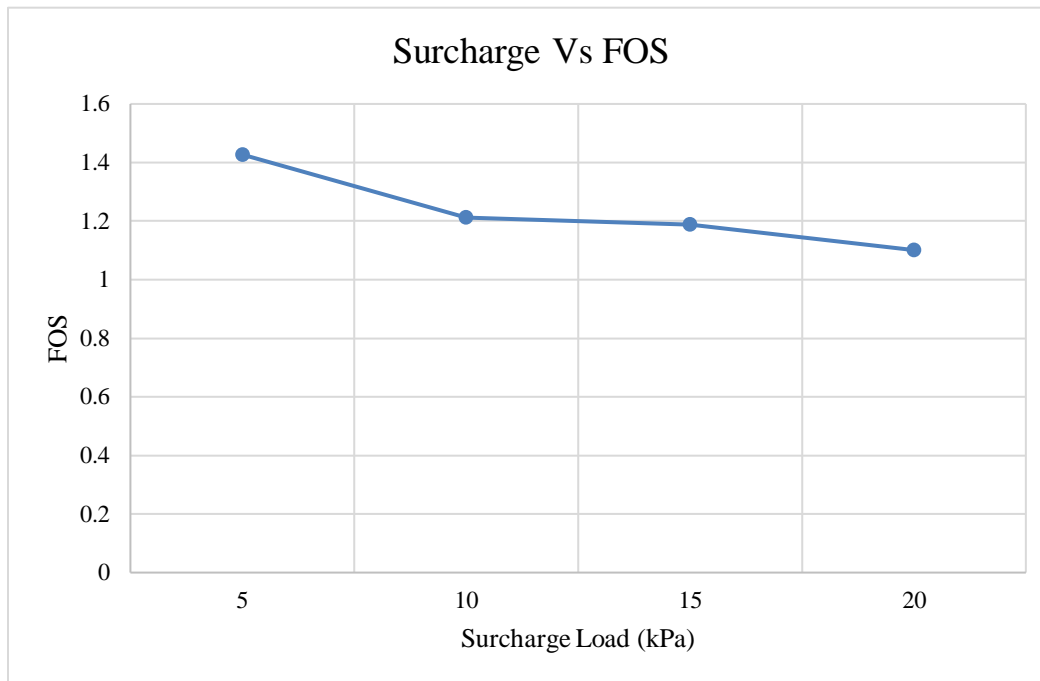
Figure 5.32: Stresses mesh with geogrids

5.2 SAFETY ANALYSIS IN PLAXIS 2D

5.2.1 Surcharge load variation with factor of safety (FOS) without geogrids in PLAXIS 2D

Table 5.1: Load variation with factor of safety without geogrids

Surcharge load (kPa)	FOS
5	1.427
10	1.212
15	1.188
20	1.101

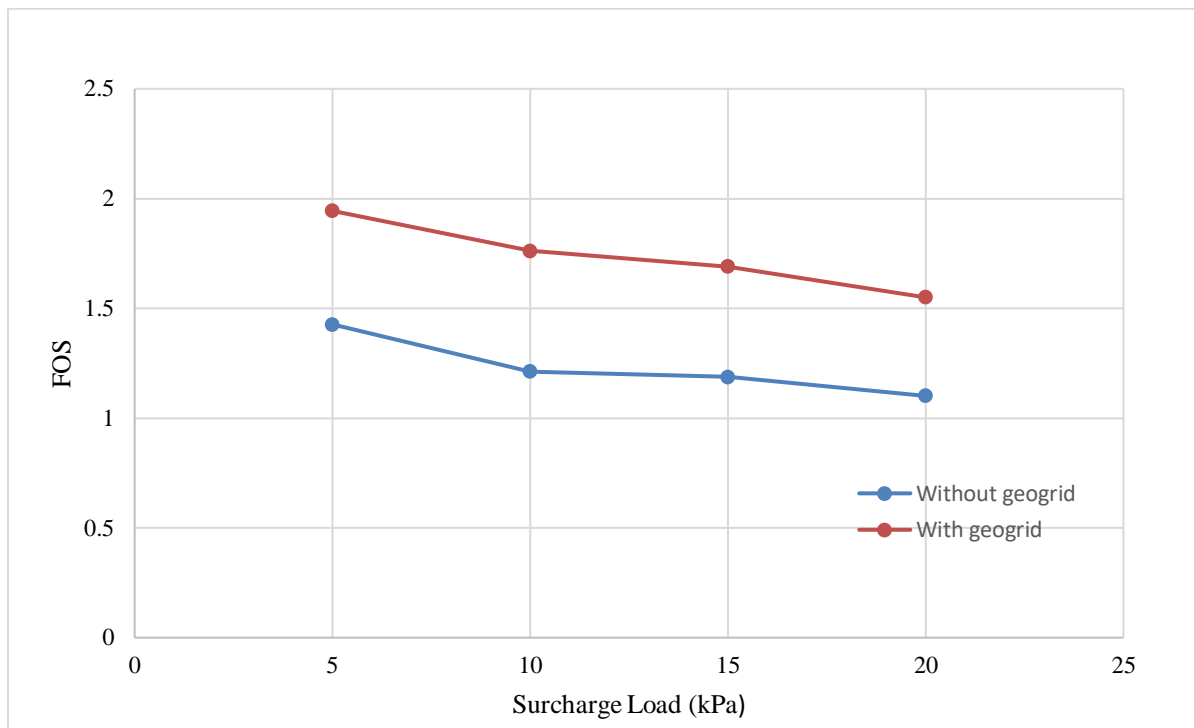


Graph 5.1: Surcharge load v/s FOS for without geogrids

5.2.2 Surcharge load variation with factor of safety (FOS) with geogrids in PLAXIS 2D

Table 5.2: Surcharge load variation with factor of safety with and without geogrid

Surcharge Load (kPa)	FOS (without Geogrid)	FOS (with geogrid)
5	1.427	1.944
10	1.212	1.762
15	1.188	1.69
20	1.101	1.55

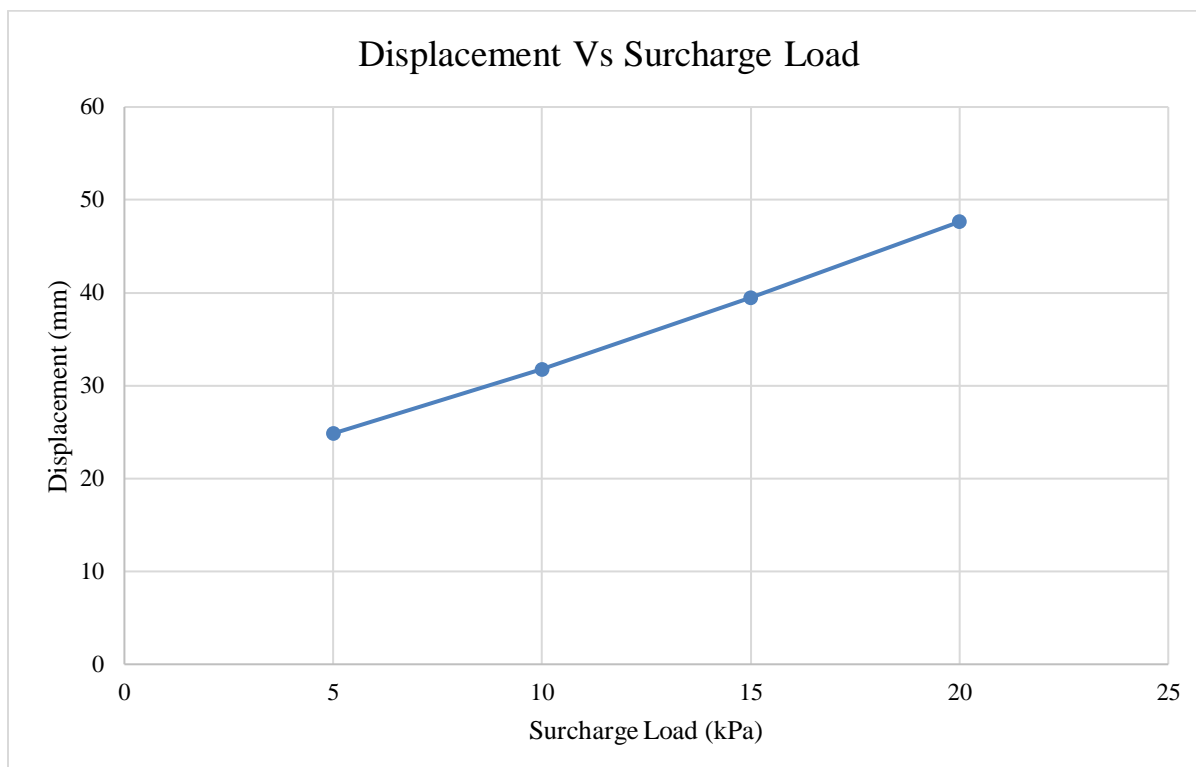


Graph 5.2: Surcharge load v/s FOS for with and without geogrid

5.2.3 Surcharge load variation with deformation without geogrids in PLAXIS 2D

Table 5.3: Surcharge load variation with displacement without geogrid

Surcharge load (kPa)	Displacement (mm)
5	24.85
10	31.74
15	39.47
20	47.64

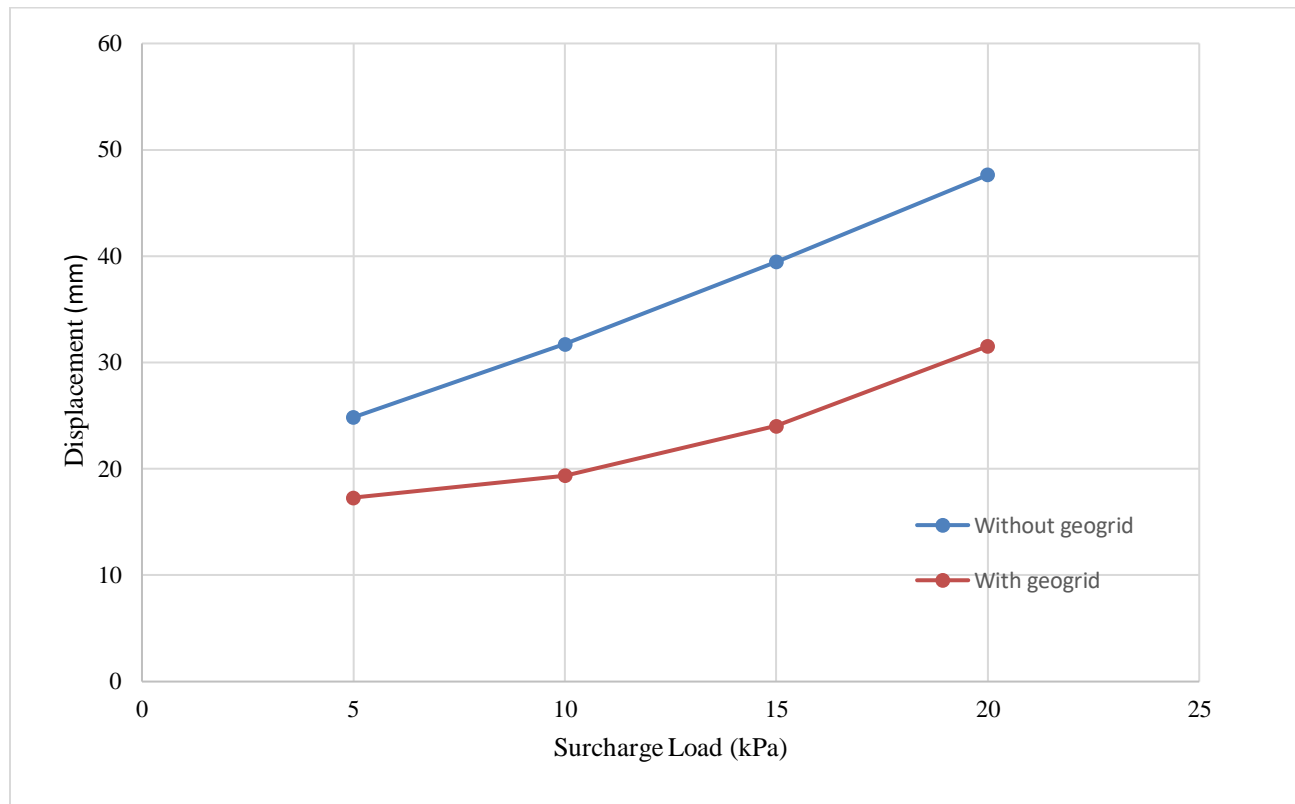


Graph 5.3: Load v/s displacement for without geogrid

5.2.3 Surcharge load variation with deformation with geogrids in PLAXIS 2D

Table 5.4 Surcharge load with displacement with geogrids

Surcharge load (kPa)	Displacement without geogrid (mm)	Displacement with geogrid (mm)
5	24.85	17.3
10	31.74	19.37
15	39.47	24.02
20	47.64	31.54

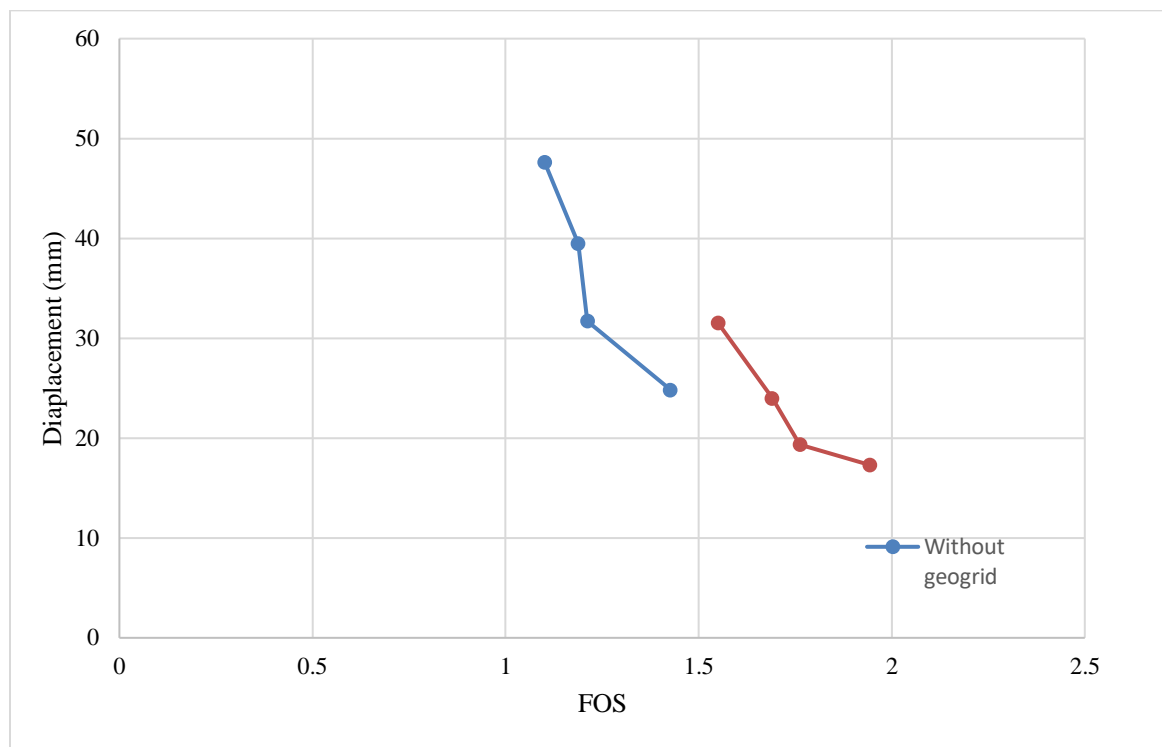


Graph 5.4: Load v/s displacement with geogrid

5.2.4 Displacement variation with factor of safety (FOS) in PLAXIS 2D

Table 5.5: Displacement variation with factor of safety with geogrid

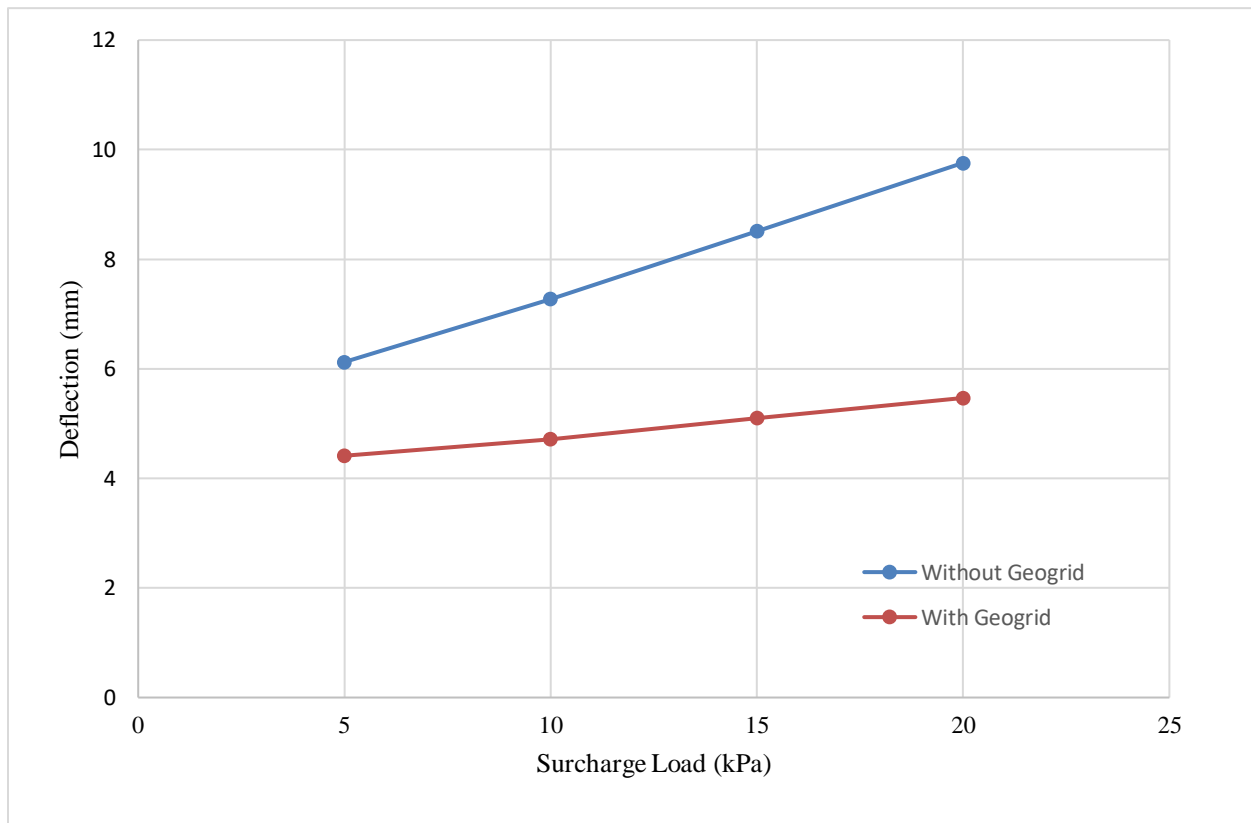
FOS	Displacement with geogrid (mm)
1.944	17.3
1.762	19.37
1.69	24.02
1.55	31.54



Graph 5.5: displacement v/s FOS with geogrid

5.2.5 Variation of displacement wall with load without and with geogrid

Surcharge Load (kPa)	Displacement in wall (without geogrid) (mm)	Displacement in wall (with geogrid) (mm)
5	6.124	4.413
10	7.273	4.717
15	8.513	5.1
20	9.759	5.468



Graph 5.6: Surcharge load v/s Deflection

DISCUSSION

From this study various conclusions are found out in PLAXIS 2D

1. From parametric study, it is found out that when load is applied on Lower GRS wall without geogrids, the value of deformation increased at higher rate and the value of factor of safety decreased at higher rate and vice versa.

When surcharge load is increased as 5kpa, 10kpa, 15kpa, 20kpa

- i. Deformation is 24.85mm, 31.74mm, 39.47mm, 47.64mm.
 - ii. Factor of safety is 1.427, 1.212, 1.188, 1.01.
 - iii. Lateral displacement is 6.124mm, 7.273mm, 8.513mm, 9.759mm.
2. When load is applied on Lower GRS wall with geogrids, the deformation is decreased and factor of safety increased.

Surcharge load is increased as 5kpa, 10kpa, 15kpa, 20kpa

- i. Deformation is decreased as 17.30mm, 19.37mm, 24.02mm, 31.54mm.
- ii. Factor of safety increased as 1.944, 1.762, 1.69, 1.55.
- iii. Lateral displacement is decreased as 4.413mm, 4.717mm, 5.10mm, 5.468mm.

Similar results have been obtained in Linhares et al. (2021), Nicks et al. (2020). The calculated results of present study are in the range of above research work.

CHAPTER 6 – CONCLUSION AND STUDY SCOPE

CONCLUSION

In this study, a series of loads is consequently applied on the wall. The resulting deformation, factor of safety and displacement for each loading case have been analysed.

After carrying out the study in plaxis 2d software, following conclusions can be drawn

- 1) The obtained value of deformation from Finite Element Analysis with Geogrids has decreased 30.38%, 43.64%, 63.85% and 64.89% respectively for the loading 5kpa, 10kpa, 15kpa and 20kpa. Results show that as the surcharge load is increased, the effectiveness of geogrids also increased. So that by providing geogrids we can reduce the deformation in backfill and can ensure safety of structure.
- 2) The obtained value of factor of safety from Finite Element Analysis with Geogrids has increased 36.22%, 45.37%, 51.81% and 57.08% respectively for the loading 5kpa, 10kpa, 15kpa and 20kpa. Factor of safety increased with use of geogrids and more effective when we increased with load, can ensure the safety of structure.
- 3) The obtained value of lateral displacement of wall from Finite Element Analysis with Geogrids has decreased 38.77%, 54.18%, 66.92% and 67.31% respectively for loading 5kpa, 10kpa, 15kpa, and 20kpa. The lateral displacement has also decreased with use Geogrids, can ensure the safety of structure.
- 4) The results of the FEM analysis correspond with the measured from case studies, the wall deformation and loads are nearly identical to the measured values. This indicates that numerical study can be employed effectively in these types of investigations.

FURTHER SCOPE OF STUDY

In the current situation, the application of the Lower GRS wall is very diverse now days. The current research focuses on the impact of various parameters on the fill material of Geogrid reinforced wall. The various situations can be considered to further study;

- We can study by taking the cohesive soil in backfill.
- By considering the settlement between the abutment and bridge.
- In this study, water table effect is not considered. Further we can consider water table in GRS wall.

REFERENCES

- 1 Mirmoradi, S. H., M. Ehrlich, and L. F. O. Magalhães. (2021). "Numerical evaluation of the effect of foundation on the behaviour of reinforced soil walls." *Geotextiles and Geomembranes* 49.3, 619-628.
- 2 Ramalakshmi, M. (2021) "Force-displacement response of bridge abutments under passive push." *Materials Today: Proceedings* 43, 883-887.
- 3 Linhares, Raquel Mariano, Seyed Hamed Mirmoradi, and Mauricio Ehrlich. (2021). "Evaluation of the effect of surcharge on the behavior of geosynthetic-reinforced soil walls." *Transportation Geotechnics* 31, 100634.
- 4 Khosrojerdi, and Mahsa. (2020). "Prediction equations for estimating maximum lateral displacement and settlement of geosynthetic reinforced soil abutments." *Computers and Geotechnics* 125, 103622.
- 5 Hatami, Kianoosh, and Ridvan Doger. (2020) "Load-bearing performance of model GRS bridge abutments with different facing and reinforcement spacing configurations." *Geotextiles and Geomembranes* 49.5, 1139-1148.
- 6 Xu, Peng, and Kianoosh Hatami. (2019). "Sliding stability and lateral displacement analysis of reinforced soil retaining walls." *Geotextiles and Geomembranes* 47.4, 483-492.
- 7 Mirmoradi, S. H., (2019). "Evaluation of the combined effect of facing inclination and uniform surcharge on GRS walls." *Geotextiles and Geomembranes* 47.5, 685-691.
- 8 Alam, Md Jahid Iftekhar, C. T. Gnanendran, and S. R. Lo. (2018) "Experimental and numerical investigations of the behaviour of footing on geosynthetic reinforced fill slope under cyclic loading." *Geotextiles and Geomembranes* 46.6, 848-859.
- 9 Zevgolis, Ioannis E., and Philippe L. Bourdeau. (2016). "Reliability and redundancy of the internal stability of reinforced soil walls." *Computers and Geotechnics* 84, 152-163.
- 10 Zheng, Yewei, and Patrick J. Fox. (2016). "Numerical investigation of geosynthetic-reinforced soil bridge abutments under static loading." *Journal of Geotechnical and Geoenvironmental Engineering* 142.5, 04016004.
- 11 Xie, Yonggui, Ben Leshchinsky, and Shangchuan Yang. (2016). "Evaluating reinforcement loading within surcharged segmental block reinforced soil walls using a limit state

- framework." *Geotextiles and Geomembranes* 44.6 (2016): 832-844.
- 12 Mirmoradi, S. H., & Ehrlich, M. (2014). Numerical evaluation of the behavior of GRS walls with segmental block facing under working stress conditions. *Journal of Geotechnical and Geoenvironmental Engineering*, 141(3), 04014109.
 - 13 Lackner, C., Bergado, D. T., & Semprich, S. (2013). Prestressed reinforced soil by geosynthetics–Concept and experimental investigations. *Geotextiles and Geomembranes*, 37, 109-123.
 - 14 Guler, E., Cicek, E., Demirkan, M. M., & Hamderi, M. (2012). Numerical analysis of reinforced soil walls with granular and cohesive backfills under cyclic loads. *Bulletin of Earthquake Engineering*, 10(3), 793-811.
 - 15 Lovisa, J., Shukla, S. K., & Sivakugan, N. (2010). Behaviour of prestressed geotextile-reinforced sand bed supporting a loaded circular footing. *Geotextiles and Geomembranes*, 28(1), 23-32.
 - 16 PLAXIS 2D–version 9.02 (2008). Reference Manual, Delft University of Technology, Delft, Netherlands.
 - 17 Guler, E., Hamderi, M., & Demirkan, M. M. (2007). Numerical analysis of reinforced soil-retaining wall structures with cohesive and granular backfills. *Geosynthetics International*, 14(6), 330-345.
 - 18 Wu, J. T., Lee, K. Z., & Pham, T. (2006). Allowable bearing pressures of bridge sills on GRS abutments with flexible facing. *Journal of Geotechnical and Geoenvironmental Engineering*, 132(7), 830-841.
 - 19 Skinner, G. D., & Rowe, R. K. (2005). Design and behaviour of a geosynthetic reinforced retaining wall and bridge abutment on a yielding foundation. *Geotextiles and Geomembranes*, 23(3), 234-260.
 - 20 Abu-Hejleh, N., Zornberg, J.G., Wang, T. and Watcharamonthein, J. (2002), “Monitored Displacements of Unique Geosynthetic-Reinforced Soil Bridge Abutments”, *Geosynthetics International*, Vol. 9, No. 1, pp. 71-95.